Msx1 deficiency interacts with hypoxia and induces

a morphogenetic regulation during lip development

Mitsushiro Nakatomi[1,2,*], Kerstin U. Ludwig[3], Michael Knapp[4], Ralf Kist[1,5], Steven Lisgo[1], Hayato Ohshima[6], Elisabeth Mangold[3], Heiko Peters[1,*]

[1] Biosciences Institute, Newcastle University, International Centre for Life, Newcastle upon Tyne, United Kingdom

[2] Division of Anatomy, Department of Health Promotion, Kyushu Dental University, Kitakyushu, Japan

[3] Institute of Human Genetics, University Hospital Bonn, Bonn, Germany

[4] Institute of Medical Biometry, Informatics and Epidemiology, University of Bonn, Bonn, Germany

[5] School of Dental Sciences, Faculty of Medical Sciences, Newcastle University, Newcastle upon Tyne, United Kingdom

[6] Division of Anatomy and Cell Biology of the Hard Tissue, Department of Tissue Regeneration and Reconstruction, Niigata University Graduate School of Medical and Dental Sciences, Niigata, Japan

* Corresponding authors: Mitsushiro Nakatomi (nktm-emb@umin.ac.jp)
Heiko Peters (heiko.peters50@gmail.com)

Development • Accepted manuscript

Summary Statement

The article describes how *Msx1* mutations cause morphological changes in the lip-forming region of mouse embryos and how this interacts with hypoxia and *Pax9* deficiency in cleft lip formation.

Abstract

Nonsyndromic clefts of the lip and palate are common birth defects resulting from gene-gene and gene-environment interactions. *MSX1* mutations have been linked to orofacial clefting and we show here that *Msx1* deficiency causes a growth defect of the medial nasal process (Mnp) in mouse embryos. While this defect alone does not disrupt lip formation, *Msx1*-deficient embryos develop a cleft lip when the mother is transiently exposed to reduced oxygen levels or to Phenytoin, a drug known to cause embryonic hypoxia. In the absence of interacting environmental factors, the Mnp growth defect caused by *Msx1*-deficiency is modified by a *Pax9*-dependent "morphogenetic regulation", which modulates Mnp shape, rescues lip formation and involves a localised abrogation of Bmp4-mediated repression of *Pax9*. Analyses of GWAS data revealed a genome-wide significant association of a Gene Ontology morphogenesis term (including assigned roles of *MSX1*, *MSX2*, *PAX9*, *BMP4*, *GREM1*) specifically for nonsyndromic cleft lip with cleft palate. Our data indicate that *MSX1* mutations may increase the risk for cleft lip formation by interacting with an impaired morphogenetic regulation that adjusts Mnp shape, or through interactions that inhibit Mnp growth.

Introduction

Clefts of the lip and palatal structures are common developmental defects in humans and are part of the phenotypic spectrum in various Mendelian syndromes (Tolarova and Cervenka, 1998). However, the majority of cleft lip and/or cleft palate (summarized as orofacial clefting) are nonsyndromic malformations and have a multifactorial aetiology, including strong contributions by interacting genetic components and environmental factors (Mossey et al., 2009). The incidence of orofacial clefting varies among different ethnic groups, gender, and socioeconomic status and occurs in 1 out of 700 births on average (Dixon et al., 2011). Based on the results of genetic and embryological studies, nonsyndromic orofacial clefts are traditionally classified as isolated, nonsyndromic cleft palate (equivalent to nonsyndromic cleft palate only, nsCPO) and nonsyndromic cleft lip that occurs with (nsCLP) or without (nsCLO) a cleft palate, the latter two collectively referred to as nsCL/P. The multifactorial aetiology and concealed Mendelian inheritance patterns underlying nsCPO and nsCL/P complicate the identification of genetic loci (Dixon et al., 2011; Seto-Salvia and Stanier, 2014), however, recent genome-wide association studies (GWAS) and meta-analyses identified at least 40 genetic risk loci for these defects (Birnbaum et al., 2009; Grant et al., 2009; Mangold et al., 2010; Beaty et al., 2010; Ludwig et al. 2012; Sun et al. 2015; Leslie et al. 2016; Ludwig et al. 2016; Ludwig et al. 2017; Yu et al., 2017; Butali et al., 2019). The studies provide an essential framework for disentangling the complex processes regulating lip and palate development (Mangold et al., 2011). However, the identity of the vast majority of causal variants and critical gene-gene (GG) and gene-environment (GE) interactions underlying the multifactorial aetiology of orofacial clefting remain to be determined.

The formation of the lip requires continuous fusion and merging of craniofacial processes (or prominences), i.e. the medial nasal process (Mnp) and the maxillary process (Mxp), both initially developing independently from each other (Gritli-Linde, 2012). A cleft of the lip occurs when this process is impaired and a cleft may extend further involving the nose when merging is disrupted also between the Mnp and the lateral nasal process (Lnp). A critically important step in lip formation is the timely regulated disintegration of the epithelium at the sites of fusion, a prerequisite for intermingling of neural crest cell-derived mesenchymal cells to establish stable

junctions. Epithelial disintegration involves programmed cell death and occurs at the so-called lambdoidal junction, the region at which the tips of Mnp, Mxp and Lnp make contact and fuse with each other. Critically important developmental pathways that regulate this tightly controlled process have been identified, showing that a *Pbx1/2*-controlled Wnt signalling pathway regulates p63/Irf6-mediated cell death in the epithelial seam at the lambdoidal junction (Ferretti et al., 2011; Kousa and Schutte, 2016). Interestingly, expanded Shh signalling negatively affects the Wnt signalling and p63/Irf6 pathways at the lambdoidal junction and results in cleft lip formation (Kurosaka et al., 2014). Expanded Shh signalling causes ectopic canonical Wnt inhibitor activity, which may involve displaced *Vax1* expression (Kurosaka et al., 2014). While functional roles of *Vax1* in lip and palate development remain to be investigated (Geoghegan et al., 2017), several reports of variants in the human *VAX1* gene highlight its involvement in human CL/P (Slavotinek et al., 2012; Butali et al., 2019).

The *MSX1* gene encodes a homeodomain-containing transcription factor, and *MSX1* haploinsufficiency in humans causes familial oligodontia (Vastardis et al., 1996). CL/P is occasionally seen in affected patients (van den Boogaard et al., 2000) and a contribution of *MSX1* mutations to nsCL/P and nsCPO was first identified by a candidate-gene linkage-disequilibrium strategy (Lidral et al., 1998). A number of studies have subsequently supported a role for *MSX1* in nonsyndromic orofacial clefting in a broad ethnic range (Fallin et al., 2003; Schultz et al., 2004; Suzuki et al., 2004; Vieira et al., 2005; Tongkobpetch et al., 2006; Otero et al., 2007; Jagomägi et al., 2010; Gowans et al., 2016) and one study suggested that about 2% of nsCL/P cases might involve mutations of the *MSX1* gene in some populations (Jezewski et al., 2003). A genome-wide significant association between genetic variants at the *MSX1* locus and the sub-phenotype nsCLP has recently been identified in the Chinese population (Yu et al., 2017). Interactions between DNA variants in *MSX1* with maternal smoking and with alcohol consumption have been suggested to increase the risk for orofacial clefting (Romitti et al., 1999; Beaty et al., 2002; Fallin et al., 2003; van den Boogaard et al., 2008), while this association was not found in a cohort of Danish origin (Mitchell et al., 2001). Likewise, a link between maternal smoking and *MSX1* variants increasing the risk for developmental limb malformations has been demonstrated (Hwang et al., 1998), but could not be confirmed by another study (Carmichael et al., 2004).

Inactivation of *Msx1* in mice results in the complete absence of teeth and cleft secondary palate (Satokata and Maas, 1994). *Msx1* and its close homolog *Msx2* are co-expressed in various craniofacial regions derived from neural crest cells, a multipotent, migratory cell population that originates from dorsal neural fold and generates a major source for skeletal and connective tissues of the developing face (Trainor, 2005; Chai and Maxson, 2006; Suzuki et al., 2016). While a cleft lip does not form in the absence of *Msx1*, *Msx1$^{-/-}$*;*Msx2$^{-/-}$* double homozygous mouse mutants exhibit severe craniofacial defects, including exencephaly and a particularly dysmorphic midface (Satokata et al., 2000; Ishii et al., 2005). In addition, defects in cardiac outflow tract formation and a severe limb phenotype in *Msx1$^{-/-}$*;*Msx2$^{-/-}$* mutants are not seen in either single mutant, showing that the functions of *Msx1* and *Msx2* can compensate for each other at various sites during development (Ishii et al., 2005; Lallemand et al., 2005). Cleft lip formation has been demonstrated to occur also in *Msx1$^{-/-}$*;*Pax9$^{-/-}$* double homozygous mouse mutants (Nakatomi et al., 2010), however, this genetic interaction has not been investigated and the impact of combined *Msx1*/*Pax9* deficiency on lip development is currently unknown.

Multiple lines of evidence have shown that episodes of embryonic hypoxia during the first trimester of human pregnancy are associated with developmental defects and craniofacial malformations, including cleft lip and palate (reviewed in Webster and Abela, 2007). More recently, an increasing number of medically relevant substances have been discovered to cause embryonic hypoxia through a significant disruption of the embryonic heart beat rate (Danielsson et al., 2003, 2005, 2007). While these adverse effects are linked to cleft lip and palate formation, their interactions with genetic predispositions in orofacial clefting are largely unknown.

RESULTS

Msx1 deficiency interacts with reduced maternal respiratory oxygen levels and with Phenytoin during lip development

Embryonic hypoxia has been implicated as an environmental risk factor for orofacial clefting (Millicovsky and Johnston, 1981a; Bronsky et al., 1986; Nagaoka et al., 2012; Smith et al., 2013). Among other causes, embryonic hypoxia may be a consequence of constriction of uterine blood vessels, or of bradycardia/arrhythmia of the embryonic heart, conditions that have been widely described as side effects of several commonly prescribed drugs (Webster and Abela, 2007). To investigate a possible interaction between *Msx1* deficiency and hypoxia we mated heterozygous *Msx1* mutant mice and exposed pregnant females to 10% O_2 during the period of early lip formation, i.e. from embryonic day (E) 10.5 to E12.5. Gross inspection of embryos at E15.5 revealed that 72% (13/18) of *Msx1* homozygous mutant embryos (*Msx1$^{-/-}$*) developed a bilateral or unilateral cleft lip, while none of the *Msx1$^{+/-}$* embryos (0/39; *P*=1.54^{-09}) or *Msx1$^{+/+}$* embryos (0/8; *P*=6.75^{-04}) showed this defect (Fig. 1A,B).

Embryonic hypoxia in the mesenchyme of the branchial arches has been identified as a side effect of Phenytoin, an anticonvulsant drug with known teratogenic effects in both humans and mice, in particular for cleft lip and cleft palate formation (Azarbayjani et al., 2001; Danielsson et al., 2005; Webster et al., 2006). Thus, to model pharmacologically induced hypoxic stress during lip development we exposed pregnant *Msx1$^{+/-}$* females to different concentrations of Phenytoin from E10.5 to E11.5. Notably, the exposure strongly increased the incidence of cleft lip formation in *Msx1$^{-/-}$* embryos in a dose-dependent manner and reached 91.7% at the highest dosage (Fig. 1C), at which all affected mutants exhibited a bilateral cleft lip. The defects involve a severe growth retardation of the developing Mnp and Mxp at E11.5 (Fig. 1D). Moreover, affected *Msx1$^{-/-}$* embryos exposed to Phenytoin at the mid-range concentration exhibited a spectrum of upper lip deformities typically seen in human patients, including hypoplastic lip, unilateral cleft lip, and bilateral cleft lip (Fig. 1E-H; Table S1). At the highest dosage, the frequency of cleft lip was increased also in heterozygous *Msx1* mutants (9.2%; *P* < 0.027; Table S1), a condition reminiscent of cleft lip formation in human patients with heterozygous mutations in *MSX1*. Consistent with redundant roles of *Msx1* and *Msx2* in craniofacial development (Ishii

et al., 2005), the sensitivity to Phenytoin-induced cleft lip was significantly increased in *Msx1*/*Msx2* compound mutants (Table S1).

To confirm the hypoxia-inducing effects of Phenytoin in the developing lip, we carried out immunohistochemical staining of Pimonidazol (Hypoxyprobe[TM]-1), which forms covalent adducts in hypoxic tissues, including mouse embryonic tissues (Arteel et al., 1995; Danielsson et al., 2003). The staining revealed a strongly increased intensity of hypoxia in the Mnp at E11.0 in both Phenytoin-treated wild-type and *Msx1*-deficient embryos, while weak staining was observed in non-treated samples (Fig. S1). In contrast, upregulated expression of Hif1, a key factor mediating vital cellular responses to embryonic hypoxia (Dunwoodie, 2009), and of the Hif1 target Vegf was less markedly upregulated in $Msx1^{-/-}$ embryos (Fig. S1). To test if it is possible to offset the adverse effects of Phenytoin during lip formation (Millicovsky and Johnston, 1981b), we kept pregnant females in a hyperoxic environment (50% O2) for the duration of Phenytoin treatment (48h). In this experimental group, only 7 out of 22 (31.8%) of the lip fusion sites were affected in *Msx1*-/- mutant embryos, while 8 out of 14 (57.1%) fusion sites showed a cleft at normoxia. While the calculated *P*-value ($P = 0.13$) did not reach statistical significance, the data suggests that simultaneous exposure to elevated oxygen levels can mitigate the adverse effects of Phenytoin on lip development in the absence of *Msx1*.

In the outbred genetic background (CD1) of the mice used in this work the interaction caused a phenotypic spectrum ranging from clefts of the soft palate only to complete cleft secondary palate (Fig. 1I-K). The interaction affects the morphogenesis of the palatal shelves (Fig. 1L) and the incidence was highly reproducible in heterozygous *Msx1* mutant embryos at higher dosages ($P<0.004$ at 60mg/kg and $P<0.0007$ at 85mg/kg, respectively) and reached 100% when *Msx1* heterozygosity was combined with the absence of *Msx2* (Fig. 1M, Table S1). Importantly, *Msx1* heterozygosity of the pregnant mother did not influence the frequency of cleft palate (Fig. S2), indicating that the genotype of the embryo is the key genetic determinant for the observed GE interactions. A GE interaction between Phenytoin and *Msx1* heterozygosity causing a cleft secondary palate was recently also observed to occur in an inbred (C57Bl/6) genetic background (M. Nakatomi, unpublished observations).

Msx1 and Pax9 regulate different aspects of Mnp development

Msx1 and *Pax9* are co-expressed in neural crest cell-derived dental mesenchyme (Mackenzie et al., 1991; Neubüser et al., 1997) and both genes are essential for tooth formation (Satokata and Maas, 1994; Chen et al., 1996; Peters et al., 1998). Moreover, *Msx1* and *Pax9* cooperatively regulate downstream target genes in the tooth mesenchyme and preliminary observations showed that about 40% of *Msx1*;*Pax9* double homozygous mouse mutants exhibited a cleft lip (Ogawa et al., 2006; Nakatomi et al., 2010). Based on these observations we speculated that the anticonvulsant drug Phenytoin might interact with *Pax9* deficiency in cleft lip formation in a similar manner to that revealed for *Msx1*. Surprisingly, however, the incidence of cleft lip of *Pax9* homozygous mutant embryos was not significantly increased at any dosage tested and there was no significant increase of Phenytoin-induced cleft palate in heterozygous *Pax9* mutant embryos (Fig. 1C; Table S1).

The strong interaction of Phenytoin with *Msx1*, but not with *Pax9*, suggests that *Msx1* and *Pax9* could regulate different aspects during lip formation. To understand this, we first compared their expression patterns in the developing Mnp, Lnp and Mxp. Whole mount *in situ* hybridization on mouse embryonic heads at E10.5 revealed that *Msx1* and *Msx2* are expressed in all three processes, while the expression of *Pax9* is restricted to the Mnp and Lnp (Fig. 2A,C,E). *In situ* hybridization on sections showed that the expression domains of *Msx1* and *Msx2* are restricted to the anterior-distal compartment of the Mnp, while *Pax9* is expressed in the posterior-proximal region of the Mnp (Fig. 2B,D,F). *In situ* hybridization of *MSX1* and immunohistochemical analyses of *PAX9* expression in human embryonic tissue revealed that both genes are expressed during human Mnp formation in patterns that are similar to those observed in mouse Mnp development (Fig. 2G-M). In addition, we found that *Msx2* and *Pax1,* the paralogous genes of *Msx1* and *Pax9*, respectively, are not upregulated in *Msx1* and *Pax9* single homozygous mutants (Fig. S3).

Next, we compared Mnp morphology of *Msx1* and *Pax9* single homozygous mutants at E11.5. At this developmental stage, the distal part of the Mnp is normally oriented towards the Lnp and Mxp (Fig. 3A), a transient and characteristic feature during mammalian upper lip formation that is also seen in primates, including humans (Senders et al., 2003). In *Msx1*$^{-/-}$ embryos, we consistently observed a growth retardation of the distal compartment of the Mnp but the contact between Mnp and

Mxp was always well established in these mutants (Fig. 3A). Importantly, this condition is associated with a considerably pronounced curvature of the Mnp (Fig. 3A,B). In contrast, the Mnp curvature is attenuated in $Pax9^{-/-}$ mutants and we did not observe a significant growth retardation of the distal Mnp region in the absence of $Pax9$ alone (Fig. 3A,B).

A Pax9-dependent alteration of Mnp morphogenesis rescues lip formation and involves up-regulated Pax9 expression in the Msx1-deficient Mnp

It is noticeable that growth retardation of the Mnp caused by *Msx1*-deficiency is consistently associated with a significant increase of the Mnp curvature. Interestingly, while the distal compartment of the Mnp was smaller also in $Msx1^{-/-};Pax9^{-/-}$ mutants, the curvature of the Mnp was significantly flattened, resulting in an irregularly long nasal pit (Fig. 3A,B). Moreover, the area of contact between Mnp and Mxp was noticeably smaller in the double homozygous mutants (Fig. 3C), resulting in a wide gap between left and right Mxp in embryos affected by cleft lip (Fig. 3D). These findings indicate that insufficient contact between Mnp and Mxp in $Msx1^{-/-};Pax9^{-/-}$ mutants resulting in a cleft lip is a consequence of combining two Mnp defects that occur independently of each other: a growth retardation caused by *Msx1* deficiency and a reduced curvature caused by the absence of *Pax9*.

Since *Pax9* deficiency leads to a decrease of the Mnp curvature we hypothesised that the establishment of a *Pax9*-dependent and pronounced Mnp curvature in $Msx1^{-/-}$ mutant embryos could involve an upregulation of *Pax9* expression. In normal Mnp development, *Pax9* is initially expressed distally but gradually becomes restricted to more proximal regions between E10.5 and E11.5 (Fig. 4A-C; Fig. S4). Interestingly, *Pax9* expression is up-regulated and distally expanded in the Mnp of $Msx1^{-/-}$ and of *Msx1/Msx2* compound mutant embryos between E10.5 and E11.5 (Fig. 4 D-F, Fig. S5). In contrast, *Msx1* expression levels are not altered in the Mnp of $Pax9^{-/-}$ mutants (Fig. 4 G,H). Together, these results show that the gradual restriction of *Pax9* expression to a proximal domain in the Mnp is *Msx1*-dependent, revealing that *Msx1* acts genetically upstream of *Pax9* in the developing Mnp.

Msx1/Msx2-regulated Bmp4 expression is involved in restricting Pax9 expression in the Mnp mesenchyme

The complementary expression patterns of *Msx1* and *Pax9* in the wild-type Mnp (Fig. 2) indicate that the *Msx1*-dependent restriction of *Pax9* expression is regulated by a non-cell autonomous mechanism. A potential candidate for mediating this process is Bmp4, a secreted growth factor that functions in a positive feedback loop with *Msx1* and *Msx2* at various sites during craniofacial development (Zhang et al., 2002) and which was shown to suppress mesenchymal *Pax9* expression in early tooth and palate development, respectively (Neubüser et al., 1997; Liu et al., 2005). In the developing Mnp, *Bmp4* expression shifts from the epithelium to the mesenchyme (Gong and Guo, 2003), where it overlaps with that of *Msx1* and *Msx2* and in which the expression pattern is complementary to that of *Pax9* at E11.0 (Fig. 4I,J). Consistent with redundant roles of *Msx1* and *Msx2* to activate mesenchymal *Bmp4* transcription, expression of *Bmp4* in the Mnp mesenchyme is strongly reduced in *Msx1*;*Msx2* compound mutants (Fig. 4K), while that of *Pax9* is expanded correspondingly (Fig. 4L). In the absence of *Msx1* alone, *Bmp4* expression is mostly affected in a medial domain within the posterior Mnp region (Fig. 4N) and expression of *Pax9* is expanded particularly into this domain. (Fig. 4P). Importantly, *Msx2* expression is barely detectable in the medial domain within the posterior Mnp in both wild type and $Msx1^{-/-}$ mutants (Fig. 4Q,R), suggesting the strong reduction of *Bmp4* expression to result from a near-complete absence of the *Msx1*/*Msx2*- regulated expression of *Bmp4* in this region. To verify a downstream effect of reduced Bmp4 signalling we analysed the distribution of phosphorylated Smad proteins (pSmad1/5/8; He et al., 2010). Quantification of pSmad1/5/8-positive nuclei revealed significantly reduced expression in the Mnp of $Msx1^{-/-}$ embryos, with 76.95% of the nuclei stained in controls, and 36.73% of the nuclei stained in $Msx1^{-/-}$ embryos (P = 0.0007, Fig. 4S-V, Fig. S6, Table S2). These results indicate that the Bmp4 downstream pathway is significantly affected in the medial area of the Mnp and supports the view that *Msx2* does not fully compensate for the absence of *Msx1* in this region.

To directly demonstrate an inhibitory effect of Bmp4 on *Pax9* expression we implanted Bmp4 protein-soaked beads into the mesenchyme of cultured nasal processes dissected at E10.5. Following organ culture, *in situ* hybridization revealed a strong down-regulation of *Pax9* in both Mnp and Lnp (Fig. 5A). This finding demonstrates that Bmp4 is sufficient for inhibiting *Pax9* expression in the Mnp mesenchyme and thus provides a plausible explanation for the expansion of *Pax9* expression seen in $Msx1^{-/-}$ and in $Msx1^{-/-};Msx2^{-/-}$ mutant embryos, respectively.

In addition to the distal expansion of *Pax9* expression seen in the Mnp of $Msx1^{-/-}$ and $Msx1^{-/-};Msx2^{-/-}$ mutant embryos we observed an increase of *Pax9* promoter activity also in the absence of a functional *Pax9* gene (Fig. 5B). This was assessed by using a combination of the non-functional *Pax9* alleles $Pax9^{LacZ}$ (Peters et al., 1998) and $Pax9^{del}$ (Kist et al., 2007), respectively. This finding indicates the presence of a negative, auto-regulatory *Pax9* feedback loop that contributes to restricting *Pax9* expression to proximal regions of the Mnp. While down-regulated Bmp4 expression likely accounts for the expanded *Pax9* expression in $Msx1^{-/-};Msx2^{-/-}$ mutant embryos, we did not detect altered *Bmp4* expression in the *Pax9*-deficient Mnp at E10.5 and E11.5 (Fig. 5C). In addition, the expression of *Shh* and its receptor *Ptch1* was not changed (M. Nakatomi, unpublished observations). However, using a candidate gene approach we found *Gremlin1* (*Grem1)*, a secreted Bmp4 antagonist (Hsu et al., 1998), to be ectopically expressed in the Mnp of $Pax9^{-/-}$ mutants (Fig. 5D). This suggests a mechanism by which up-regulated *Grem1* expression neutralizes Bmp4-mediated inhibition of *Pax9* expression in the MNP mesenchyme of $Pax9^{-/-}$ mutants.

Collectively, the data suggest a model that integrates *Msx1* and *Pax9* functions into two parallel acting pathways that are connected through a relay mechanism involving Bmp4 (Fig. 5E). Whereas *Msx1* is primarily required for Mnp growth, a loss of *Msx1* function also causes decreased Bmp4 expression, which lowers Bmp4-mediated repression of *Pax9*. Our data suggest that the resulting increase of *Pax9* activity induces a morphogenetic regulation and an adjustment of Mnp shape that facilitates contact with the Mxp.

Genome-wide significant association of "organ morphogenesis" (GO:0009887) for nsCLP includes MSX1, MSX2, PAX9, BMP4, and GREM1.

To investigate if genetic data from genome-wide association studies (GWAS) in human nsCL/P samples support our model of morphogenetic regulation derived from the experimental animal work (Fig 5E), we turned to large-cohort data from human patients with nsCL/P and its subtypes nsCLP and nsCLO. We retrieved GWAS data from a previously published meta-analysis (Ludwig et al., 2017) and performed both single-gene and pathway-analyses. First, we tested for association in aggregate of common variants in the genes investigated in this study, and each of the three traits as listed above. A set-based test as implemented in VEGAS (Liu et al., 2010) was applied to imputed data of both a European (Euro) and a multiethnic (All) meta-analysis. Consistent with previous results (Ludwig et al., 2016), *GREM1* reached genome-wide significance for nsCL/P and nsCLP (Table 1). We also observed a test-wide significant enrichment for *MSX1* in nsCL/P, and additional nominally significant results for all remaining genes and nsCL/P, except for *BMP4*. While the significant associations of *MSX1* and *MSX2* are reflected by contributions from both nsCLP and nsCLO, the significance in nsCL/P for *PAX9* is primarily driven by nsCLP only (with non-significant results for nsCLO, Table 1).

Prompted by these results we investigated whether GWAS association signals are overrepresented in aggregate in Gene Ontology (GO) pathways that include *MSX1*, *PAX9*, *BMP4*, and *GREM1*. Using gene-based *P*-values generated above, we carried out individual VEGAS pathway analyses for nsCL/P, nsCLP and nsCLO. In the analysis of nsCLP, a genome-wide significant result was identified for "organ morphogenesis" (GO:0009887), with $P=1\times10^{-06}$ after 10^6 permutations. Repeating the analysis with 10^7 permutations revealed $P=2\times10^{-07}$. When performed for nsCLO, the pathway-based result for GO:0009887 was not significant ($P>0.5$). The morphogenesis pathway GO:0009887 also includes *MSX2*, and a total of 557 genes directly matched results of the nsCLP-specific VEGAS pathway analysis (Table S3), whereas 75 genes identified by the VEGAS pathway analysis did not produce a match in GO:0009887 (Table S4). Interestingly, a substantial proportion of these genes (185 out of 632; 29.3%) has previously been reported to play a role for human or mouse orofacial clefting, or for facial development (Tables S3, S4). Moreover, GO:0009887

was recently identified also through a data base search approach for genes involved in jaw morphogenesis and disorders (Manocha et al., 2018).

We finally investigated whether the morphogenesis pathway GO:0009887 also plays a role in normal facial variation. Based on a list of 112 genes located at genetic loci previously identified to be associated with diverse facial traits through GWAS (Liu et al., 2012; Paternoster et al., 2012; Adhikari et al., 2016; Cole et al., 2016; Pickrell et al., 2016; Shaffer et al., 2016; Cha et al., 2018; Claes et al., 2018; Indencleef et al., 2018; Xiong et al., 2019), we identified 37 genes that were among the 632 genes included in GO:0009887 (33%, Table S5). Statistical assessment of whether the overlap between both gene sets was significant, revealed a highly significant P-value ($P<10^{-16}$, hypergeometric test), suggesting that the morphogenesis pathway also contributes to variation of facial traits in the general population.

DISCUSSION

Interaction between Msx1 deficiency and hypoxia increases the risk for orofacial clefting

Our data show that transient exposure of pregnant mice to reduced respiratory oxygen levels during a critical time-period of lip development is sufficient to cause cleft lip in $Msx1^{-/-}$ mouse embryos at an incidence of about 72% (0% cleft lip in $Msx1^{-/-}$ embryos at normoxia), whereas none of the wild-type embryos showed this defect. In addition, more than 50% of $Msx1^{-/-}$ embryos developed a cleft lip when the pregnant mouse was injected with 60 mg/kg Phenytoin (90% cleft lip at 85 mg/kg). In contrast, the incidence of cleft lip was extremely low in wild-type embryos (0% at 60 mg/kg Phenytoin and 2% at 85 mg/kg Phenytoin, respectively), consistent with previous results showing that CD1 mice are particularly resistant to the teratogenic effects of Phenytoin (Hansen and Hodes, 1983; Azarbayjani et al., 2006). Together, the data reveals a strong, and specific, GE interaction involving deficiency of $Msx1$ and transient hypoxia, which could be relevant also in the aetiology of orofacial clefting in humans.

Interestingly, low oxygen partial pressure is present at high altitude, which has been suggested to underlie an increased risk for cleft lip formation in Bolivia (Castilla et al., 1999) and may be a factor contributing to an increased risk for orofacial clefting

in certain regions in China (Fan et al., 2018). Other conditions linked to orofacial clefting in humans may induce embryonic hypoxia during pregnancy also at normoxia, including constriction of uterine vessels, placental insufficiency, and life style factors such as smoking (Webster and Abela, 2007). Moreover, various pharmacologically relevant substances used in the treatment of epilepsy have been suggested to cause hypoxia directly in the developing embryo (Danielsson et al., 2007). The anticonvulsant drug Phenytoin represents an example of this group and our results clearly demonstrate that *Msx1* deficiency in mouse embryos greatly enhances the susceptibility to the cleft lip-inducing effects of Phenytoin. A high sensitivity to reduced *Msx1* gene dosage is also illustrated in $Msx1^{+/-}$ mutants with different genetic backgrounds, which may form a cleft secondary palate at a high frequency when exposed to Phenytoin (Fig.1; M. Nakatomi, unpublished observations). Previous work showed that combined *Msx1/Msx2* deficiency is associated with impaired maturation of the endothelial layer of blood vessels, a defect secondary to the abnormal development of neural crest-derived vascular smooth muscle cells (Lopes et al., 2011). Similarly, $Msx1^{-/-}$ embryos show transiently impaired blood vessel formation during facial development (Medio et al., 2012). Our data showing reduced upregulation of the hypoxia marker Hif1 and Vegf in *Msx1*-deficient Mnp exposed to Phenytoin are consistent with these findings.

Additional research is warranted to investigate the molecular basis for the interaction between *Msx1* deficiency and Phenytoin-induced hypoxia. Phenytoin is considered to cause irregular phases of embryonic hypoxia, which are followed by episodes of re-oxygenation and the formation of reactive oxygen species (Danielsson et al., 2007). *Msx1* may be involved in oxidative stress response, however, the strong interaction between *Msx1* deficiency and a continuous exposure to reduced maternal oxygen levels argues that additional mechanism should be considered, too.

Phenytoin was shown to inhibit a voltage-dependent K^+ channel (I_{kr}) that is expressed in the developing rodent heart. I_{kr} is encoded by an *ether-a-go-go-related* gene and is particularly sensitive during the period of heart development that coincides with critical stages of lip and palate formation (Danielson et al., 2005). Interestingly, I_{kr} blocking activities have been demonstrated for several antiarrhythmics, but also for some antihistamines, antibiotics and antipsychotic drugs (Tarmago et al., 2004). With regards to orofacial clefting, epidemiological analyses have not yet produced conclusive data on the roles of these drugs. However, since

these analyses were carried out on samples collected from a genetically highly heterogenous population, it is conceivable that inconclusive results and low risk estimates might mask significantly increased risks in those patients that are genetically predisposed. Nevertheless, our results revealed that mutations in *Msx1* strongly interact with hypoxic stress during mouse lip development and the findings may therefore be useful for an improved risk assessment in patient groups affected by heterozygous mutations in *MSX1*: these patients are regularly affected by oligodontia (Fournier et al., 2018), a phenotype that is readily diagnosed and thus could be helpful to aid the development of targeted prevention strategies, e.g. during the early period of pregnancy.

Msx1-deficiency induces a Pax9-dependent morphogenetic regulation

Identifying causative GE and GG interactions that underlie non-syndromic forms of orofacial clefting in humans is a complex challenge. Although mutations in *MSX1* are frequently associated with nsCL/P, these birth defects are incompletely penetrant and phenotypes are highly variable across individuals within affected families (Gu et al., 2018). Previous work has shown that absence of *Msx1* and *Msx2* in mouse embryos results in severely growth-retarded craniofacial processes (Ishii et al., 2005), defects that clearly predispose to cleft palate and cleft lip. Here we show that a reduction of Mnp size is associated with a moderate but significant alteration of Mnp shape (Fig 2), a finding that has not been described before. The enhanced curvature of the Mnp appears to facilitate contact with the Mxp to complete lip formation. We propose the capacity of the Mnp to react to a growth retardation by inducing a favourable alteration of Mnp shape to represent a "morphogenetic regulation": when compared to midfacial development of other mammals, the evolutionary shortening of the maxilla and depressed midfacial anatomy typically seen in primates, in particular in the hominid clade (Lacruz et al., 2019), requires that the growth of their midfacial area is naturally suppressed during development. It is therefore tempting to speculate that a morphogenetic regulation that compensates for a genetically caused growth defect may be critically important specifically in humans. Our data suggest that a morphogenetic regulation could present a significant component of the "developmental robustness" of lip formation in humans; its disruption may therefore be considered as a novel, pathogenic mechanism in the aetiology of cleft lip.

The morphogenetic regulation enhancing the Mnp curvature in *Msx1*$^{-/-}$ embryos is *Pax9*-dependent and provides a mechanistic explanation for the negative epistasis between *Msx1* and *Pax9* in lip development. The lack of a distinct Mnp curvature in *Pax9*-deficient embryos is reminiscent of a morphogenetic disruption of the secondary palatal shelves in these mutants; similar to the Mnp, the secondary palatal shelves are not growth retarded but show a distinct absence of indentations on the oral side (Peters et al., 1998; Zhou et al., 2013; Jia et al., 2017). Both Mnp and palatal shelves of *Pax9*$^{-/-}$ mutant embryos appear bulky and uniformly shaped, defects that clearly reveal an important role for *Pax9* in the morphogenesis of both structures during a critical period of development. With respect to lip formation, we show that the expression domain of *Pax9* in the Mnp is controlled by *Msx1* and involves *Msx1*-regulated expression of *Bmp4*. Interestingly, the shift of *Bmp4* expression from the epithelium to the mesenchyme (Gong and Guo, 2003) correlates with the gradual restriction of *Pax9* expression to the proximal region of the developing Mnp by Bmp4. Together, the interactions involving *Msx1*, *Pax9*, *Bmp4*, and *Grem1* may contribute to a molecular network that continuously coordinates growth and shape of the Mnp during a critical period of lip development (Fig. 5E). While the functions of *Grem1* in Mnp morphogenesis remain to be tested *in vivo* using appropriate genetic modelling, important roles for *GREM1* in human nose and lip development have been indicated by a strong association between polymorphisms at the *GREM1* locus and nose width (Boehringer et al., 2011), and by genome-wide significant associations between variants at the *GREM1* locus and nsCLP (Ludwig et al., 2016) and other forms of orofacial clefting (Gowans et al., 2018; Wang et al., 2018; Rafighdoost et al. 2019).

The mechanism by which *Pax9* controls the morphogenesis of the Mnp remain to be elucidated. *Pax9* might be involved in regulating differential growth directly within different areas in the Mnp. The function of *Pax9* may also affect Mnp development by regulating the growth of the primary palate, which could contribute to a lateral displacement of the distal regions of the Mnp and is affected in *Pax9*$^{-/-}$ embryos (Jia et al., 2017; Li et al., 2017). Moreover, the irregular and extended nasal pit in *Pax9*$^{-/-}$ mutant embryos may indicate that *Pax9* is required also for regulating efficient epithelial fusion between Mnp and Lnp at the lambdoid junction. Interestingly, Wnt-signalling has been shown to play a critical role in this process (Ferretti et al., 2011; reviewed in Reynolds et al., 2019) and inhibition of secreted

antagonists of Wnt signalling has been demonstrated to be sufficient to rescue cleft palate in *Pax9*-deficient mouse embryos (Jia et al., 2017; Li et al., 2017).

Orofacial clefts and facial morphogenesis

GWAS have established significant associations of regions around *MSX1*, *PAX9*, and *GREM1* in the aetiology of orofacial clefts in humans of different ethnic origins (Yu et al., 2017; Huang et al., 2019; Ludwig et al., 2016; Table 1). While genome-wide significance for loci around *BMP4* and *MSX2* in human orofacial clefting remains yet to be demonstrated, analyses of mouse mutant embryos have shown that, except for *Grem1*, all five genes regulate the development of both secondary palate and lip (Satokata and Maas, 1994; Liu et al., 2005; Suzuki et al. 2009; Nakatomi et al., 2010, Parada and Chai, 2012; Ludwig et al., 2016; this work). Interestingly, our pathway analysis identified a genome-wide significant overrepresentation of common DNA variants in the "organ morphogenesis" for nsCLP and not nsCPO, which points to a particular importance of the genes, in particular those analysed in this study, in this specific orofacial clefting sub-phenotype. The genome-wide significance of the *MSX1* locus for nsCLP (Yu et al., 2017) supports this view.

Regarding lip development, our data suggest that all five genes studied in this work may participate in a genetic network that controls Mnp morphogenesis during a critical period of lip formation in mice (Fig. 5E). While overt clefts of the lip represent a clinically relevant outcome of impaired lip development in humans, more subtle genetic alterations are increasingly recognised to manifest as milder phenotypes affecting lip and mid-facial morphology in the non-affected population (Boehringer et al., 2011; Liu et al., 2012; Miller et al., 2014; Wilson-Nagrani et al., 2018; Xiong et al., 2019). Our comparison identified a considerable overlap between genes identified in the "organ morphogenesis" pathway and those associated with facial variations, thus supporting the concept of shared genetic effects on orofacial clefting and variations of facial development.

Materials and methods

Mice

All experimental procedures were carried out under a project license evaluated by the Newcastle University Local Ethics Committee and approved by the Home Office (UK), the Institutional Animal Care and Use Committee of Niigata University and the Kyushu Dental University Animal Care and Use Committee. Single heterozygous mice of *Msx1* (Satokata and Maas, 1994) were maintained on a CD1 (Newcastle Univ.) or C57BL/6 (Niigata Univ. and Kyushu Dental Univ.) genetic background, respectively. Wild type or *Msx1*$^{+/-}$ mice were used as controls. Single heterozygous mice of *Pax9* (Peters et al., 1998) and *Msx2* (Satokata et al., 2000) and combined double heterozygous mice of *Pax9;Msx1* and *Msx1;Msx2* were maintained on a CD1 background, while *Pax9*^{flox} and *PGK-Cre* mice (Kist et al., 2007; Lallemand et al., 1998) were propagated on a C57BL/6 background. The day of vaginal plug detection was designated as embryonic day (E) 0.5. At least three samples of each genotype were collected and analysed.

Human foetal sections

Human foetal tissue sections were obtained from the MRC/Wellcome-Trust funded Human Developmental Biology Resource at Newcastle University (HBDR, http://www.hdbr.org), with appropriate maternal written consent and with approval from the Newcastle and North Tyneside NHS Health Authority Joint Ethics Committee. HDBR is a licenced research tissue bank with the UK Human Tissue Authority.

Whole-mount and section in situ hybridization

Embryos were dissected and fixed with 4% Paraformaldehyde (PFA) in Phosphate Buffered Saline (PBS) at 4 ºC for overnight. For whole-mount *in situ* hybridization, samples were dehydrated through a graded series of methanol. For section *in situ* hybridization and immunohistochemistry, samples were dehydrated through a graded series of ethanol and xylene, embedded in paraffin and cut into 4 µm frontal sections. Non-radioactive whole-mount and section *in situ* hybridizations were carried out as previously described (Nakatomi et al., 2010). The *MSX1 in situ* probe was generated by PCR amplification using SP6 and T7 tagged primers (AATACGATTTAGGTGACACTATAGAATACGTGCCTCT GGCCCCTTCCAGCGCG; TAAGTTAATACGACTCACTATAGGGCGAACATA GTACACACAATCCCTTCCA).

Immunohistochemistry

For immunohistochemical analysis, sections were treated with anti-phospho-Smad1/5 primary antibody (rabbit monoclonal, #9516, Cell Signaling Technology, Danvers, MA, USA; 1:200 dilution), anti-rabbit secondary antibody (#BA-1000, Vector Laboratories, Burlingame, CA, USA; 1:500 dilution) and Vectastain Elite ABC kit (Vector; 1:50 dilution), essentially according to the manufacturers' instructions. Sigmafast 3, 3'-diaminobenzidine (DAB) tablets (Sigma-Aldrich, St Louis, MO, USA) were used for colour reaction, followed by counterstaining with diluted hematoxylin. Negative control experiment replacing primary antibody with PBS did not yield significant staining. For cell counting, a 200 x 50 µm rectangle was set at the mesial corner of the mesial nasal process, where *Msx1* is intensely expressed, of both right and left sides of three serial sections (in total six rectangles per individual) using Adobe Photoshop CS software (Adobe Systems, San Jose, CA, USA). The ratio of DAB positive cells/total cells in the rectangle was measured using ImmunoRatio free web application (https://biii.eu/immunoratio; Tuominen et al., 2010). The average of six rectangles was calculated to obtain a pSmad score of each individual area and Student's *t*-test (two-tailed) was carried out to compare controls with $Msx1^{-/-}$ mutant embryos (n = 4 each). PAX9 immunostaining on human sections was carried out as previously described (Kist et al., 2014) using DAB as a chromogen.

Phenytoin experiments

Phenytoin (PHT) injection was performed as previously reported (Azarbayjani et al., 2001). Briefly, PHT sodium salt (Sigma-Aldrich) was freshly dissolved in 0.9% NaCl (pH11.7) and intraperitoneally injected to pregnant $Msx1^{+/-}$ mice (CD1 background) at 11 am at both E10.5 and 11.5 at different concentrations (35, 60 and 85 mg / kg body weight, respectively). Embryos were dissected at E15.5 and fixed with Bouin's fixative after recording facial cleft state. Chi-square test was carried out for statistical analysis regarding the occurrence of cleft lip between wild-type (N=98, 85mg/kg; 39, 60mg/kg; 28, 35mg/kg) and $Msx1^{-/-}$ (N=12, 85mg/kg; 19, 60mg/kg; 18, 35mg/kg) embryos. To label hypoxic cells, pimonidazole (60 mg / kg body weight) contained in a Hypoxyprobe-1 Plus Kit (Hypoxyprobe, Inc., Burlington, MA, USA) was intraperitoneally injected to pregnant mice 1 h before sacrifice at E11.5 after PHT injection as described above. Labelled cells in frontally cut paraffin sections were immunohistochemically visualized using primary antibody (anti-FITC-MAb1; 1:100

dilution), secondary antibody (HRP conjugated rabbit anti-FITC; 1:400 dilution) and DAB tablets (Sigma-Aldrich), followed by counterstaining with diluted hematoxylin.

Hypoxic chamber experiment

For hypoxia experiments, pregnant $Msx1^{+/-}$ mice (C57BL/6 background) were kept in an airtight chamber (Deuce Co., Ltd., Tokyo, Japan) in which the O_2 concentration was maintained at 10% for 48 h from E10.5 to 12.5. The oxygen concentration was continuously monitored with an oxygen analyser (JKO-25MT II R, Ichinen Jikco Ltd., Tokyo, Japan). Then embryos were dissected at E15.5 and fixed with Bouin's fixative to analyse lip phenotype. Chi-square test was carried out for statistical analysis regarding the occurrence of cleft lip between wild-type (N=3) and $Msx1^{-/-}$ (N=8) embryos.

Rescue experiment

To examine whether hyperoxic environment can rescue PHT-induced cleft lip, pregnant $Msx1^{+/-}$ mice (C57BL/6 background) were injected with PHT (60 mg / kg) once a day at E10.5 and 11.5 and kept at 50% O_2 concentration in the airtight chamber for 48 h from E10.5 to 12.5. The oxygen concentration was continuously monitored with the oxygen analyzer. Then embryos were dissected at E15.5 and fixed with Bouin's fixative to analyse lip phenotype. PHT injection on pregnant $Msx1^{+/-}$ mice (C57BL/6 background) with the same condition in normoxic environment was performed as control. Chi-square test was carried out for statistical analysis regarding the occurrence of cleft lip between normoxic (N=7) and hyperoxic (N=11) groups of $Msx1^{-/-}$.

Whole-mount X-gal staining

Dissected embryos were fixed with 1% Formaldehyde in PBS containing 0.02% NP-40 (PBS-NP) at 4 ℃ for 20 minutes. Samples were washed with PBS-NP at room temperature for 15 minutes 3 times and incubated with staining buffer (2 mM $MgCl_2$, 5 mM $K_4Fe(CN)_6 \cdot 3H_2O$, 5 mM $K_3Fe(CN)_6$ and 1 mg/ml X-gal in PBS-NP) at 37 ℃ for overnight, followed by several rinses with PBS .

Scanning electron microscopy (SEM) and morphometric measurements

Embryos were dissected and fixed with 2% Glutaraldehyde in Sorenson's Phosphate Buffer at 4 °C for overnight. Following tissue processing and SEM were carried out according to a standard protocol at Electron Microscopy Research Services, Newcastle University, UK. The oral and nasal angles of the medial nasal process were measured by using Adobe Photoshop CS software (Adobe Systems). N = 42 (WT), 16 ($Msx1^{-/-}$), 14 ($Pax9^{-/-}$) and 17 ($Msx1^{-/-};Pax9^{-/-}$). Student's *t*-test (two-tailed) was performed for the comparison of the oral or nasal angles.

Organ culture

Affi-gel blue beads (Bio-Rad Laboratories, USA) were soaked with 500 µg/ml human recombinant BMP4 protein (R&D Systems, USA) or control PBS. Mouse embryos (E10.5) were harvested and facial regions were dissected prior to bead implantation into the Mnp. Samples were cultured by Trowel's standard method with Dulbecco's Modified Eagles Medium (SIGMA-ALDRICH, USA) including antibiotics and 10% Foetal Bovine Serum. After 8 hours, cultured wild-type samples were fixed with 4% PFA for whole mount *in situ* hybridization, while $Pax9^{+/LacZ}$ samples were fixed with 1% PFA in PBS for X-gal staining.

Gene-based association and pathway analysis

To test for association between each trait (nsCL/P, nsCLO and nsCLP) and common SNPs in each of the genes considered in this study (*MSX1, MSX2, BMP4, PAX9, GREM1*), a set-based test implemented in VEGAS2 (Liu et al. 2010) was performed (script accessed at https://vegas2.qimrberghofer.edu.au/, January 2017). To this end, we used our previous in-house meta-analysis data (Ludwig et al., 2017), which contained imputed data for nsCL/P, nsCLP and nsCLO. For each of the five genes, we extracted *P*-values for all common variants at the respective genetic loci (± 50 kb, minor allele frequency > 1%, info-score > 0.4) and calculated whether there is an enrichment of SNPs with significant association *P*-values, while accounting for linkage disequilibrium (LD) between markers. An empirical *P*-value for the 10% top SNPs was calculated as the proportion of permutated test statistics less than the observed test statistics in each gene, with the numbers of permutations increasing depending on the *P*-value obtained.

To identify pathways in which genes with significant *P*-values from this gene-based test were overrepresented, an adapted version of VEGAS2 (VEGAS2-pathway analysis) was used. For this, gene-based *P*-values were calculated for all RefSeq genes and used as input. This tool additionally requires a „gene-pathway annotation" file, in which GO-pathways are defined and genes are assigned to those pathways. For the present analysis, we used the "Biosystems gene-pathway annotation file" as available at the VEGAS2 homepage (January 2017). PubMed and OMIM databases available at the National Centre for Biotechnology Information platform (www.ncbi.nlm.nih.gov/) were used to search for genes with documented roles in lip, palate, and facial development.

References

Adhikari, K., Fuentes-Guajardo, M., Quinto-Sánchez, M., Mendoza-Revilla, J., Camilo Chacón-Duque, J., Acuña-Alonzo, V., Jaramillo, C., Arias, W., Lozano, R.B., Pérez, G.M. et al. (2016). A genome-wide association scan implicates *DCHS2*, *RUNX2*, *GLI3*, *PAX1* and *EDAR* in human facial variation. *Nat. Commun.* **7**, 11616. doi: 10.1038/ncomms11616.

Arteel, G.E., Thurman, R.G., Yates, J.M. and Raleigh, J.A. (1995). Evidence that hypoxia markers detect oxygen gradients in liver: pimonidazole and retrograde perfusion of rat liver. *Br. J. Cancer* **72**, 889-895.

Azarbayjani, F. and Danielsson, B.R. (2001). Phenytoin-induced cleft palate: evidence for embryonic cardiac bradyarrhythmia due to inhibition of delayed rectifier K+ channels resulting in hypoxia-reoxygenation damage. *Teratology* **63**, 152-160.

Azarbayjani, F., Borg, L.A. and Danielsson, B.R. (2006). Increased susceptibility to phenytoin teratogenicity: excessive generation of reactive oxygen species or impaired antioxidant defense? *Basic Clin. Pharmacol. Toxicol.* **99**, 305-311.

Beaty, T.H., Hetmanski, J.B., Zeiger, J.S., Fan, Y.T., Liang, K.Y., VanderKolk, C.A. and McIntosh, I. (2002). Testing candidate genes for non-syndromic oral clefts using a case-parent trio design. *Genet. Epidemiol.* **22**, 1-11.

Beaty, T.H., Murray, J.C., Marazita, M.L., Munger, R.G., Ruczinski, I., Hetmanski, J.B., Liang, K.Y., Wu, T., Murray, T. and Fallin, M.D. et al. (2010). A genome-wide association study of cleft lip with and without cleft palate identifies risk variants near MAFB and ABCA4. *Nat. Genet.* **42**, 525-529.

Birnbaum, S., Ludwig, K.U., Reutter, H., Herms, S., Steffens, M., Rubini, M., Baluardo, C., Ferrian, M., Almeida de Assis, N. and Alblas, M.A. et al. (2009). Key susceptibility locus for nonsyndromic cleft lip with or without cleft palate on chromosome 8q24. *Nat. Genet.* **41**, 473-477.

Bronsky, P.T., Johnston, M.C. and Sulik, K.K. (1986). Morphogenesis of hypoxia-induced cleft lip in CL/Fr mice. *J. Craniofac. Genet. Dev. Biol. Suppl.* **2**, 113-128.

Butali, A., Mossey, P.A., Adeyemo, W.L., Eshete, M.A., Gowans, L.J.J., Busch, T.D., Jain, D., Yu, W., Huan, L. and Laurie, C.A. et al. (2019). Genomic analyses in African populations identify novel risk loci for cleft palate. *Hum. Mol. Genet.* **28**, 1038-1051.

Boehringer, S., van der Lijn, F., Liu, F., Günther, M., Sinigerova, S., Nowak, S., Ludwig, K.U., Herberz, R., Klein, S., Hofman, A. et al. (2011). Genetic determination of human facial morphology: links between cleft-lips and normal variation. *Eur. J. Hum. Genet.* **19**, 1192-1197.

Butali, A., Mossey, P.A., Adeyemo, W.L., Eshete, M.A., Gowans, L.J.J., Busch, T.D., Jain, D., Yu, W., Huan, L., Laurie, C.A. (2019). Genomic analyses in African populations identify novel risk loci for cleft palate. *Hum. Mol. Genet.* **28**, 1038-1051.

Carmichael, S.L., Shaw, G.M., Yang, W., Lammer, E.J., Zhu, H. and Finnell R.H. (2004). Limb deficiency defects, *MSX1*, and exposure to tobacco smoke. *Am. J. Med. Genet. A.* **125A**, 285-289.

Castilla, E.E., Lopez-Camelo, J.S. and Campaña, H. (1999). Altitude as a risk factor for congenital anomalies. *Am. J. Med. Genet*. **86**, 9-14.

Cha, S., Lim, J.E., Park, A.Y., Do, J.H., Lee, S.W., Shin, C., Cho, N.H., Kang, J.O., Nam, J.M., Kim, J.S. et al. (2018). Identification of five novel genetic loci related to facial morphology by genome-wide association studies. *BMC Genomics* **19**, 481. doi: 10.1186/s12864-018-4865-9.

Chai, Y. and Maxson, R.E. Jr. (2006). Recent advances in craniofacial morphogenesis. *Dev. Dyn.* **235**, 2353-2375.

Chen, Y., Bei, M., Woo, I., Satokata, I. and Maas, R. (1996). *Msx1* controls inductive signaling in mammalian tooth morphogenesis. *Development*. **122**, 3035-3044.

Claes, P., Roosenboom, J., White, J.D., Swigut, T., Sero, D., Li, J., Lee, M.K., Zaidi, A., Mattern, B.C., Liebowitz C. et al. (2018). Genome-wide mapping of global-to-local genetic effects on human facial shape. *Nat. Genet.* **50**, 414-423.

Cole, J.B., Manyama, M., Kimwaga, E., Mathayo, J., Larson, J.R., Liberton, D.K., Lukowiak, K., Ferrara, T.M., Riccardi, S.L., Li, M. et al. (2016). Genomewide association study of African children identifies association of *SCHIP1* and *PDE8A* with facial size and shape. *PLoS Genet.***12**, e1006174. doi: 10.1371/journal.pgen.1006174.

Danielsson, B.R., Sköld, A.C., Johansson, A., Dillner, B. and Blomgren, B. (2003). Teratogenicity by the hERG potassium channel blocking drug almokalant: use of hypoxia marker gives evidence for a hypoxia-related mechanism mediated via embryonic arrhythmia. *Toxicol. Appl. Pharmacol.* **193**, 168-176.

Danielsson, B.R., Johansson, A., Danielsson, C., Azarbayjani, F., Blomgren, B. and Sköld, A.C. (2005). Phenytoin teratogenicity: hypoxia marker and effects on embryonic heart rhythm suggest an hERG-related mechanism. *Birth Defects Res. A Clin. Mol. Teratol.* **73**, 146-153.

Danielsson, B.R., Lansdell, K., Patmore, L. and Tomson, T. (2005). Effects of the antiepileptic drugs lamotrigine, topiramate and gabapentin on hERG potassium currents. *Epilepsy Res.* **63**, 17-25.

Danielsson, B.R., Danielsson, C. and Nilsson, M.F. (2007). Embryonic cardiac arrhythmia and generation of reactive oxygen species: common teratogenic mechanism for IKr blocking drugs. *Reprod Toxicol*. **24**, 42-56.

Dixon, M.J., Marazita, M.L., Beaty, T.H. and Murray, J.C. (2011). Cleft lip and palate: understanding genetic and environmental influences. *Nat. Rev. Genet.* **12**, 167-178.

Dunwoodie, S.L. (2009). The role of hypoxia in development of the Mammalian embryo. *Dev. Cell* **17**, 755-773.

Fallin, M.D., Hetmanski, J.B., Park, J., Scott, A.F., Ingersoll, R., Fuernkranz, H.A., McIntosh, I. and Beaty, T.H. (2003). Family-based analysis of *MSX1* haplotypes for association with oral clefts. *Genet. Epidemiol.* **25**, 168-175.

Fan, D., Wu, S., Liu, L., Xia, Q., Tian, G., Wang, W., Ye, S., Wang, L., Rao, J., Yang, X. et al. (2018). Prevalence of non-syndromic orofacial clefts: based on 15,094,978 Chinese perinatal infants. *Oncotarget* **9**, 13981-13990.

Ferretti, E., Li, B., Zewdu, R., Wells, V., Hebert, J.M., Karner, C., Anderson, M.J., Williams, T., Dixon, J., Dixon, M.J. et al. (2011). A conserved Pbx-Wnt-p63-Irf6 regulatory module controls face morphogenesis by promoting epithelial apoptosis. *Dev. Cell* **21**, 627-641.

Fournier, B.P., Bruneau, M.H., Toupenay, S., Kerner, S., Berdal, A., Cormier-Daire, V., Hadj-Rabia, S., Coudert, A.E. and de La Dure-Molla, M. (2018). Patterns of Dental Agenesis Highlight the Nature of the Causative Mutated Genes. *J. Dent. Res.* **97**, 1306-1316.

Geoghegan. F,, Xavier, G.M., Birjandi, A.A., Seppala, M. and Cobourne, M.T. (2017). Vax1 plays an indirect role in the etiology of murine cleft palate. *J. Dent. Res.* **96**, 1555-1562.

Gong, S.G. and Guo, C. (2003). *Bmp4* gene is expressed at the putative site of fusion in the midfacial region. *Differentiation* **71**, 228-236.

Gowans, L.J., Adeyemo, W.L., Eshete, M., Mossey, P.A., Busch, T., Aregbesola, B., Donkor, P., Arthur, F.K., Bello, S.A., Martinez, A. et al. (2016). Association studies and direct DNA sequencing implicate genetic susceptibility loci in the etiology of nonsyndromic orofacial clefts in sub-Saharan African populations. *J. Dent. Res.* **95**, 1245-1256.

Gowans, L.J.J., Oseni, G., Mossey, P.A., Adeyemo, W.L., Eshete, M.A., Busch, T.D., Donkor, P., Obiri-Yeboah, S., Plange-Rhule, G., Oti, A.A. et al. (2018). Novel *GREM1* variations in sub-Saharan African patients with cleft lip and/or cleft palate. *Cleft Palate Craniofac. J.* **55**, 736-742.

Grant, S.F., Wang, K., Zhang, H., Glaberson, W., Annaiah, K., Kim, C.E., Bradfield, J.P., Glessner, J.T., Thomas, K.A., Garris, M. et al. (2009). A genome-wide association study identifies a locus for nonsyndromic cleft lip with or without cleft palate on 8q24. *J. Pediatr.* **155**, 909-913.

Gritli-Linde, A. (2012). The mouse as a developmental model for cleft lip and palate research. *Front. Oral Biol.* **16**, 32-51.

Gu, M., Zhang, Y., Liu, H., Liu, J., Zhu, D. and Yang, X. (2018). *MSH homeobox 1* polymorphisms and the risk of non-syndromic orofacial clefts: a meta-analysis. *Eur. J. Oral Sci.* **126**, 180-185.

Hansen, D.K. and Hodes, M.E. (1983). Comparative teratogenicity of phenytoin among several inbred strains of mice. *Teratology* **28**, 175-179.

He, F., Xiong, W., Wang, Y., Matsui, M., Yu, X., Chai, Y., Klingensmith, J. and Chen, Y. (2010). Modulation of BMP signaling by Noggin is required for the maintenance of palatal epithelial integrity during palatogenesis. *Dev. Biol.* **347**, 109-121.

Hsu, D.R., Economides, A.N., Wang, X., Eimon, P.M. and Harland, R.M. (1998). The Xenopus dorsalizing factor Gremlin identifies a novel family of secreted proteins that antagonize BMP activities. *Mol. Cell* **1**, 673-683.

Hwang, S.J., Beaty, T.H., McIntosh, I., Hefferon, T. and Panny, S.R. (1998). Association between homeobox-containing gene *MSX1* and the occurrence of limb deficiency. *Am. J. Med. Genet.* **75**, 419-423.

Indencleef, K., Roosenboom, J., Hoskens, H., White, J.D., Shriver, M.D., Richmond, S., Peeters, H., Feingold, E., Marazita, M.L., Shaffer, J.R. et al. (2018). Six NSCL/P loci show associations with normal-range craniofacial variation. *Front Genet.* **9**, 502. doi: 10.3389/fgene.2018.00502.

Ishii, M., Han, J., Yen, H.Y., Sucov, H.M., Chai, Y. and Maxson, R.E. Jr. (2005). Combined deficiencies of *Msx1* and *Msx2* cause impaired patterning and survival of the cranial neural crest. *Development* **132**, 4937-4950.

Jagomägi, T., Nikopensius, T., Krjutskov, K., Tammekivi, V., Viltrop, T., Saag, M. and Metspalu, A. (2010). *MTHFR* and *MSX1* contribute to the risk of nonsyndromic cleft lip/palate. *Eur. J. Oral Sci.* **118**, 213-220.

Jezewski, P.A., Vieira, A.R., Nishimura, C., Ludwig, B., Johnson, M., O'Brien, S.E., Daack-Hirsch, S., Schultz, R.E., Weber, A., Nepomucena, B. et al. (2003). Complete sequencing shows a role for *MSX1* in non-syndromic cleft lip and palate. *J. Med. Genet*. **40**, 399-407.

Jia, S., Zhou, J., Fanelli, C., Wee, Y., Bonds, J., Schneider, P., Mues, G. and D'Souza, R.N. (2017). Small-molecule Wnt agonists correct cleft palates in *Pax9* mutant mice *in utero*. *Development* **144**, 3819-3828.

Kist, R., Greally, E. and Peters, H. (2007). Derivation of a mouse model for conditional inactivation of *Pax9*. *Genesis* **45**, 460-464.

Kist, R., Watson, M., Crosier, M., Robinson, M., Fuchs, J., Reichelt, J. and Peters, H. (2014). The formation of endoderm-derived taste sensory organs requires a *Pax9*-dependent expansion of embryonic taste bud progenitor cells. *PLoS Genet.* **10**, e1004709. doi: 10.1371/journal.pgen.1004709

Kousa, Y.A. and Schutte, B.C. (2016). Toward an orofacial gene regulatory network. *Dev. Dyn.* **245**, 220-232.

Lacruz, R.S., Stringer, C.B., Kimbel, W.H., Wood, B., Harvati, K., O'Higgins, P., Bromage, T.G. and Arsuaga, J.L. (2019). The evolutionary history of the human face. *Nat. Ecol. Evol.* **3**, 726-736.

Lallemand, Y., Luria, V., Haffner-Krausz, R. and Lonai, P. (1998). Maternally expressed PGK-Cre transgene as a tool for early and uniform activation of the Cre site-specific recombinase. *Transgenic Res.* **7**, 105-112.

Lallemand, Y., Nicola, M.A., Ramos, C., Bach, A., Cloment, C.S. and Robert, B. (2005). Analysis of *Msx1*; *Msx2* double mutants reveals multiple roles for *Msx* genes in limb development. *Development* **132**, 3003-3014.

Leslie, E.J., Carlson, J.C., Shaffer, J.R., Feingold, E., Wehby, G., Laurie, C.A., Jain, D., Laurie, C.C., Doheny, K.F., McHenry, T. et al. (2016). A multi-ethnic genome-wide association study identifies novel loci for non-syndromic cleft lip with or without cleft palate on 2p24.2, 17q23 and 19q13. *Hum. Mol. Genet.* **25**, 2862-2872.

Li, C., Lan, Y., Krumlauf, R. and Jiang, R. (2017). Modulating Wnt signaling rescues palate morphogenesis in *Pax9* mutant mice. *J. Dent. Res.* **96**, 1273-1281.

Lidral, A.C., Romitti, P.A., Basart, A.M., Doetschman, T., Leysens, N.J., Daack-Hirsch, S., Semina, E.V., Johnson, L.R., Machida, J., Burds, A. et al. (1998). Association of *MSX1* and *TGFB3* with nonsyndromic clefting in humans. *Am. J. Hum. Genet.* **63**, 557-568.

Liu, W., Sun, X., Braut, A., Mishina, Y., Behringer, R.R., Mina, M. and Martin, J.F. (2005). Distinct functions for Bmp signaling in lip and palate fusion in mice. *Development* **132**, 1453-1461.

Liu, J.Z., McRae, A.F., Nyholt, D.R., Medland, S.E., Wray, N.R., Brown, K.M, AMFS Investigators, Hayward, N.K., Montgomery, G.W., Visscher, P.M. et al. (2010). A versatile gene-based test for genome-wide association studies. *Am. J. Hum. Genet.* **87**, 139-145.

Liu, F., van der Lijn, F., Schurmann, C., Zhu, G., Chakravarty, M.M., Hysi, P.G., Wollstein, A., Lao, O., de Bruijne, M., Ikram, M.A. et al. (2012). A genome-wide association study identifies five loci influencing facial morphology in Europeans. *PLoS Genet.* **8**, e1002932. doi: 10.1371/journal.pgen.1002932.

Lopes, M., Goupille, O., Saint Cloment, C., Lallemand, Y., Cumano, A. and Robert, B. (2011). *Msx* genes define a population of mural cell precursors required for head blood vessel maturation. *Development* **138**, 3055-3066.

Ludwig, K.U., Mangold, E., Herms, S., Nowak, S., Reutter, H., Paul, A., Becker, J., Herberz, R., AlChawa, T., Nasser, E. et al. (2012). Genome-wide meta-analyses of nonsyndromic cleft lip with or without cleft palate identify six new risk loci. *Nat. Genet.* **44**, 968-971.

Ludwig, K.U., Ahmed, S.T., Böhmer, A.C., Sangani, N.B., Varghese, S., Klamt, J., Schuenke, H., Gültepe, P., Hofmann, A., Rubini, M. et al. (2016). Meta-analysis reveals genome-wide significance at 15q13 for nonsyndromic clefting of both the lip and the palate, and functional analyses implicate *GREM1* as a plausible causative gene. *PLoS Genet*. **12**, e1005914. doi: 10.1371/journal.pgen.1005914.

Ludwig, K.U., Böhmer, A.C., Bowes, J., Nikolic, M., Ishorst, N., Wyatt, N., Hammond, N.L., Gölz, L., Thieme, F., Barth, S. et al. (2017). Imputation of orofacial clefting data identifies novel risk loci and sheds light on the genetic background of cleft lip ± cleft palate and cleft palate only. *Hum. Mol. Genet*. **26**, 829-842.

Mackenzie, A., Leeming, G.L., Jowett, A.K., Ferguson, M.W. and Sharpe, P.T. (1991). The homeobox gene *Hox 7.1* has specific regional and temporal expression patterns during early murine craniofacial embryogenesis, especially tooth development in vivo and in vitro. *Development* **111**, 269-285.

Mangold, E., Ludwig, K.U., Birnbaum, S., Baluardo, C., Ferrian, M., Herms, S., Reutter, H., de Assis, N.A., Chawa, T.A., Mattheisen M. et al. (2010). Genome-wide association study identifies two susceptibility loci for nonsyndromic cleft lip with or without cleft palate. *Nat. Genet*. **42**, 24-26.

Mangold, E., Ludwig, K.U. and Nöthen, M.M. (2011). Breakthroughs in the genetics of orofacial clefting. *Trends Mol. Med.* **17**, 725-733.

Manocha, S., Farokhnia, N., Khosropanah, S., Bertol, J.W., Santiago, J. Junior, and Fakhouri, W.D. (2019). Systematic review of hormonal and genetic factors involved in the nonsyndromic disorders of the lower jaw. *Dev Dyn*. **248**, 162-172.

Medio, M., Yeh, E., Popelut, A., Babajko, S., Berdal, A. and Helms, J.A. (2012). Wnt/β-catenin signaling and *Msx1* promote outgrowth of the maxillary prominences. *Front. Physiol.* 3:375. doi: 10.3389/fphys.2012.00375.

Miller, S.F., Weinberg, S.M., Nidey, N.L., Defay, D.K., Marazita, M.L., Wehby, G.L. and Moreno Uribe, L.M. (2014). Exploratory genotype-phenotype correlations of facial form and asymmetry in unaffected relatives of children with non-syndromic cleft lip and/or palate. *J. Anat.* **224**, 688-709.

Millicovsky, G. and Johnston, M.C. (1981). Maternal hyperoxia greatly reduces the incidence of phenytoin-induced cleft lip and palate in A/J mice. *Science* **212**, 671-672.

Millicovsky, G. and Johnston, M.C. (1981). Hyperoxia and hypoxia in pregnancy: simple experimental manipulation alters the incidence of cleft lip and palate in CL/Fr mice. *Proc. Natl. Acad. Sci. U S A* **78**, 5722-5723.

Mitchell, L.E., Murray, J.C., O'Brien, S. and Christensen, K. (2001). Evaluation of two putative susceptibility loci for oral clefts in the Danish population. *Am. J. Epidemiol.* **153**, 1007-1015.

Mossey, P.A., Little, J., Munger, R.G., Dixon, M.J. and Shaw, W.C. (2009). Cleft lip and palate. *Lancet* **374**, 1773-1785.

Nagaoka, R., Okuhara, S., Sato, Y., Amagasa, T. and Iseki, S. (2012). Effects of embryonic hypoxia on lip formation. *Birth. Defects Res. A Clin. Mol. Teratol.* **94**, 215-222.

Nakatomi, M., Wang, X.P., Key, D., Lund, J.J., Turbe-Doan, A., Kist, R., Aw, A., Chen, Y., Maas, R.L. and Peters, H. (2010). Genetic interactions between *Pax9* and *Msx1* regulate lip development and several stages of tooth morphogenesis. *Dev. Biol.* **340**, 438-449.

Neubüser, A., Koseki, H. and Balling, R. (1995). Characterization and developmental expression of *Pax9*, a paired-box-containing gene related to *Pax1*. *Dev. Biol.* **170**, 701-716.

Neubüser, A., Peters, H., Balling, R. and Martin, G.R. (1997). Antagonistic interactions between FGF and BMP signaling pathways: a mechanism for positioning the sites of tooth formation. *Cell*. **90**, 247-255.

Ogawa, T., Kapadia, H., Feng, J.Q., Raghow, R., Peters, H. and D'Souza, R.N. (2006). Functional consequences of interactions between Pax9 and Msx1 genes in normal and abnormal tooth development. *J Biol Chem*. **281**, 18363-18369.

Otero, L., Gutiérrez, S., Cháves, M., Vargas, C. and Bérmudez, L. (2007). Association of *MSX1* with nonsyndromic cleft lip and palate in a Colombian population. *Cleft Palate Craniofac. J.* **44**, 653-656.

Parada, C. and Chai, Y. (2012). Roles of BMP signaling pathway in lip and palate development. *Front. Oral Biol.* **16**, 60-70.

Paternoster, L., Zhurov, A.I., Toma, A.M., Kemp, J.P., St Pourcain, B., Timpson, N.J., McMahon, G., McArdle, W., Ring, S.M., Smith, G.D. et al. (2012). Genome-wide association study of three-dimensional facial morphology identifies a variant in *PAX3* associated with nasion position. *Am. J. Hum. Genet*. **90**, 478-485.

Peters, H., Neubüser, A., Kratochwil, K. and Balling, R. (1998). *Pax9*-deficient mice lack pharyngeal pouch derivatives and teeth and exhibit craniofacial and limb abnormalities. *Genes Dev.* **12**, 2735-2747.

Pickrell, J.K., Berisa, T., Liu, J.Z., Ségurel, L., Tung, J.Y. and Hinds, D.A. (2016). Detection and interpretation of shared genetic influences on 42 human traits. *Nat. Genet.* **48**, 709-717.

Rafighdoost, H., Poudineh, A., Bahari, G., Ghaffari, H. and Hashemi, M. (2019). Association of Genetic Polymorphisms of *GREM1* Gene with Susceptibility to Non-Syndromic Cleft Lip with or without Cleft Palate in an Iranian Population. *Fetal Pediatr. Pathol.* **25**, 1-13.

Reynolds, K., Kumari, P., Sepulveda Rincon, L., Gu, R., Ji, Y., Kumar, S. and Zhou, C.J. (2019). Wnt signaling in orofacial clefts: crosstalk, pathogenesis and models. *Dis. Model. Mech*. **12**. doi: 10.1242/dmm.037051.

Romitti, P.A., Lidral, A.C., Munger, R.G., Daack-Hirsch, S., Burns, T.L., Murray, J.C. (1999). Candidate genes for nonsyndromic cleft lip and palate and maternal cigarette smoking and alcohol consumption: evaluation of genotype-environment interactions from a population-based case-control study of orofacial clefts. *Teratology*. **59**, 39-50.

Satokata, I. and Maas, R. (1994). *Msx1* deficient mice exhibit cleft palate and abnormalities of craniofacial and tooth development. *Nat. Genet.* **6**, 348-356.

Satokata, I., Ma, L., Ohshima, H., Bei, M., Woo, I., Nishizawa, K., Maeda, T., Takano, Y., Uchiyama, M., Heaney, S. et al. (2000). *Msx2* deficiency in mice causes pleiotropic defects in bone growth and ectodermal organ formation. *Nat. Genet.* **24**, 391-395.

Schultz, R.E., Cooper, M.E., Daack-Hirsch, S., Shi, M., Nepomucena, B., Graf, K.A., O'Brien, E.K., O'Brien, S.E., Marazita, M.L. and Murray, J.C. (2004). Targeted scan of fifteen regions for nonsyndromic cleft lip and palate in Filipino families. *Am. J. Med. Genet A*. **125A**, 17-22.

Senders, C.W., Peterson, E.C., Hendrickx, A.G. and Cukierski, M.A. (2003). Development of the upper lip. *Arch. Facial Plast. Surg*. **5**, 16-25.

Setó-Salvia, N. and Stanier, P. (2014). Genetics of cleft lip and/or cleft palate: association with other common anomalies. *Eur. J. Med. Genet.* **57**, 381-393.

Shaffer, J.R., Orlova, E., Lee, M.K., Leslie, E.J., Raffensperger, Z.D., Heike, C.L., Cunningham, M.L., Hecht, J.T., Kau, C.H., Nidey, N.L. et al. (2016). Genome-wide association study reveals multiple loci influencing normal human facial morphology. *PLoS Genet*. **12**, e1006149. doi: 10.1371/journal.pgen.1006149.

Slavotinek, A.M., Chao, R., Vacik, T., Yahyavi, M., Abouzeid, H., Bardakjian, T., Schneider, A., Shaw, G., Sherr, E.H., Lemke, G., Youssef, M., Schorderet, D.F. et al (2012). VAX1 mutation associated with microphthalmia, corpus callosum agenesis, and orofacial clefting: the first description of a VAX1 phenotype in humans. *Hum. Mutat.* **33**, 364-368.

Smith, F., Hu, D., Young, N.M., Lainoff, A.J., Jamniczky, H.A., Maltepe, E., Hallgrimsson, B. and Marcucio, R.S. (2013). The effect of hypoxia on facial shape variation and disease phenotypes in chicken embryos. *Dis. Model. Mech*. **6**, 915–924.

Sun, Y., Huang, Y., Yin, A., Pan, Y., Wang, Y., Wang, C., Du, Y., Wang, M., Lan, F., Hu, Z. et al. (2015). Genome-wide association study identifies a new susceptibility locus for cleft lip with or without a cleft palate. *Nat. Commun.* **16**, 6414.

Suzuki, Y., Jezewski, P.A., Machida, J., Watanabe, Y., Shi, M., Cooper, M.E., Viet le, T., Nguyen, T.D., Hai, H., Natsume, N. et al. (2004). In a Vietnamese population, *MSX1* variants contribute to cleft lip and palate. *Genet. Med.* **6**, 117-125.

Suzuki, S., Marazita, M.L., Cooper, M.E., Miwa, N., Hing, A., Jugessur, A., Natsume, N., Shimozato, K., Ohbayashi, N., Suzuki, Y. et al. (2009). Mutations in *BMP4* are associated with subepithelial, microform, and overt cleft lip. *Am. J. Hum. Genet.* **84**, 406-411.

Suzuki, A., Sangani, D.R., Ansari, A. and Iwata, J. (2016). Molecular mechanisms of midfacial developmental defects. *Dev. Dyn.* **245**, 276-293.

Tamargo, J., Caballero, R., Gómez, R., Valenzuela, C. and Delpón, E. (2004). Pharmacology of cardiac potassium channels. *Cardiovasc. Res.* **62**, 9-33.

Tolarová, M.M. and Cervenka, J. (1998). Classification and birth prevalence of orofacial clefts. *Am. J. Med. Genet.* **75**, 126-137.

Tongkobpetch, S., Siriwan, P. and Shotelersuk, V. (2006). *MSX1* mutations contribute to nonsyndromic cleft lip in a Thai population. *J. Hum. Genet.* **51**, 671-676.

Trainor, P.A. (2005). Specification of neural crest cell formation and migration in mouse embryos. *Semin. Cell. Dev. Biol.* **16**, 683-693.

Tuominen, V.J., Ruotoistenmäki, S., Viitanen, A., Jumppanen, M. and Isola, J. (2010). ImmunoRatio: a publicly available web application for quantitative image analysis of estrogen receptor (ER), progesterone receptor (PR), and Ki-67. *Breast Cancer Res.* **12**, R56. doi: 10.1186/bcr2615.

van den Boogaard, M.J., Dorland, M., Beemer, F.A. and van Amstel, H.K. (2000). *MSX1* mutation is associated with orofacial clefting and tooth agenesis in humans. *Nat. Genet.* **24**, 342-343.

van den Boogaard, M.J., de Costa, D., Krapels, I.P., Liu, F., van Duijn, C., Sinke, R.J., Lindhout, D. and Steegers-Theunissen, R.P. (2008). The *MSX1* allele 4 homozygous child exposed to smoking at periconception is most sensitive in developing nonsyndromic orofacial clefts. *Hum. Genet.* **124**, 525-534.

Vastardis, H., Karimbux, N., Guthua, S.W., Seidman, J.G. and Seidman, C.E. (1996). A human *MSX1* homeodomain missense mutation causes selective tooth agenesis. *Nat. Genet.* **13**, 417-421.

Vieira, A.R., Avila, J.R., Daack-Hirsch, S., Dragan, E., Félix, T.M., Rahimov, F., Harrington, J., Schultz, R.R., Watanabe, Y., Johnson, M. et al. (2005). Medical sequencing of candidate genes for nonsyndromic cleft lip and palate. *PLoS Genet.* **1**, e64. doi: 10.1371/journal.pgen.0010064.

Wang, X., Song, H., Jiao, X., Hao, Y., Zhang, W., Gao, Y., Li, Y., Mi, N. and Yan, J. (2018). Association between a single-nucleotide polymorphism in the *GREM1* gene and non-syndromic orofacial cleft in the Chinese population. *J. Oral Pathol. Med*. **47**, 206-210.

Webster, W.S., Howe, A.M., Abela, D. and Oakes, D.J. (2006). The relationship between cleft lip, maxillary hypoplasia, hypoxia and phenytoin. *Curr. Pharm. Des*. **12**, 1431-1448.

Webster, W.S. and Abela, D. (2007). The effect of hypoxia in development. *Birth Defects Res. C Embryo. Today*. **81**, 215-228.

Wilson-Nagrani, C., Richmond, S. and Paternoster, L. (2018). Non-syndromic cleft lip and palate polymorphisms affect normal lip morphology. *Front. Genet.* **9**, 413. doi: 10.3389/fgene.2018.00413.

Xiong, Z., Dankova, G., Howe, L.J., Lee, M.K., Hysi, P.G., de Jong, M.A., Zhu, G., Adhikari, K., Li, D., Li, Y. et al. (2019). Novel genetic loci affecting facial shape variation in humans. *Elife* **8**, pii: e49898. doi: 10.7554/eLife.49898.

Yu, Y., Zuo, X., He, M., Gao, J., Fu, Y., Qin, C., Meng, L., Wang, W., Song, Y., Cheng, Y. et al. (2017). Genome-wide analyses of non-syndromic cleft lip with palate identify 14 novel loci and genetic heterogeneity. *Nat. Commun.* **8**, 14364. doi: 10.1038/ncomms14364.

Zhang, Z., Song, Y., Zhao, X., Zhang, X., Fermin, C. and Chen, Y. (2002). Rescue of cleft palate in *Msx1*-deficient mice by transgenic Bmp4 reveals a network of BMP and Shh signaling in the regulation of mammalian palatogenesis. *Development* **129**, 4135-4146.

Zhou, J., Gao, Y., Lan, Y., Jia, S. and Jiang, R. (2013). *Pax9* regulates a molecular network involving Bmp4, Fgf10, Shh signaling and the Osr2 transcription factor to control palate morphogenesis. *Development* **140**, 4709-4718.

Table 1: Gene-based tests in genome-wide data on nonsyndromic cleft lip with or without cleft palate and its two main subtypes

Gene	Region [a]	Type [b]	nsCL/P			nsCLP			nsCLO		
			N	P-value [c]	Per	N	P-value [c]	Per	N	P-value [c]	Per
MSX1	Chr 4: 4811391 - 4915660	Euro	1241	0.011	*	1235	0.042	*	1286	0.341	-
		All		7.67×10^{-04}	**		0.045	*		0.020	*
MSX2	Chr 5: 174101575 - 174207902	Euro	852	0.029	*	855	0.058	*	863	0.003	*
		All		0.029	*		0.053	*		0.014	*
PAX9	Chr 14: 37076772 - 37197011	Euro	885	0.090	*	864	0.027	*	886	0.511	-
		All		0.043	*		0.018	*		0.513	-
GREM1	Chr 15: 32960204 - 33076870	Euro	905	2.00×10^{-06}	**	894	2.00×10^{-06}	**	941	0.209	-
		All		3.10×10^{-05}	**		6.00×10^{-06}	**		0.457	-
BMP4	Chr 14: 54366454 - 54473554	Euro	678	0.105	-	683	0.337	-	685	0.608	-
		All		0.347	-		0.727	-		0.198	-

Chr: Chromosome; N: Number of SNPs; Per: number of permutations

[a] Analysis included 50 kb up-and downstream of longest transcript, according to hg19.

[b] as described in Ludwig et al 2017.

[c] VEGAS empirical *P*-values are genome-wide significant if lower than 2×10^{-06} after 10^{6} simulations. Shaded in grey if nominally significant

* Asterisks denote number of permutations performed (no asterisk: 10^{3}, * 10^{5}, ** 10^{6} permutations);
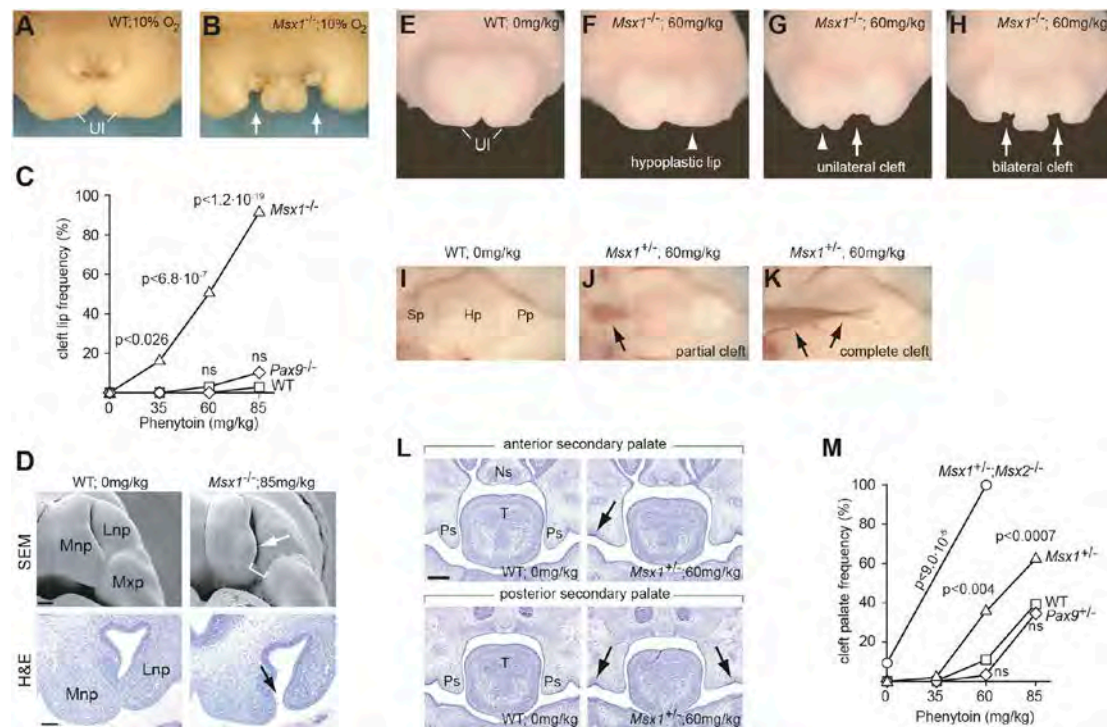
Figures

Fig. 1. *Msx1* interacts with low oxygen level and Phenytoin in orofacial clefting
(**A,B**) Upper lip development is not affected in E15.5 wild-type (WT) embryos after transient exposure of the pregnant female to 10% O2 (**A**), while *Msx1*$^{-/-}$ embryos frequently develop a bilateral cleft lip (**B**). (**C**) Injection of Phenytoin causes unilateral or bilateral cleft lip formation in *Msx1*$^{-/-}$ embryos in a dose-dependent manner. Deficiency of *Pax9* does not result in a significant increase of cleft lip. (**D**) Scanning electron microscopy (SEM) images and sections stained with hematoxylin/eosin (H&E) at E11.5. *Msx1*-deficient embryos exhibit a wide gap between Mnp and Mxp (bracket) and a cleft between Mnp and Lnp (arrows) following injection of Phenytoin. (**E-H**) Phenytoin injections cause a range of upper lip malformations in *Msx1*$^{-/-}$ embryos (**F-G**). (**I-K**) Oral view of secondary palate at E15.5. Phenytoin-treated *Msx1*$^{+/-}$ embryos may develop a partial (**J**) or complete cleft (**K**). (**L**) Frontal sections of Phenytoin-treated *Msx1*$^{+/-}$ embryos (E13.5) occasionally lack indentations of the palatal shelves (arrows). (**M**) *Msx2*-deficiency increases the frequency of cleft palate when combined with *Msx1* heterozygosity, while *Pax9* heterozygosity does not interact with Phenytoin in cleft palate formation. Abbreviations: Hp, hard palate; Lnp, lateral nasal process; Mnp, medial nasal process;

Mxp, maxillary process; Ns, Nasal septum; ns, not significant; Pp, primary palate; Ps, palatal shelves; Sp, soft palate; T, tongue; UL, upper lip. Scale bars: 100μm (D), 200μm (L).
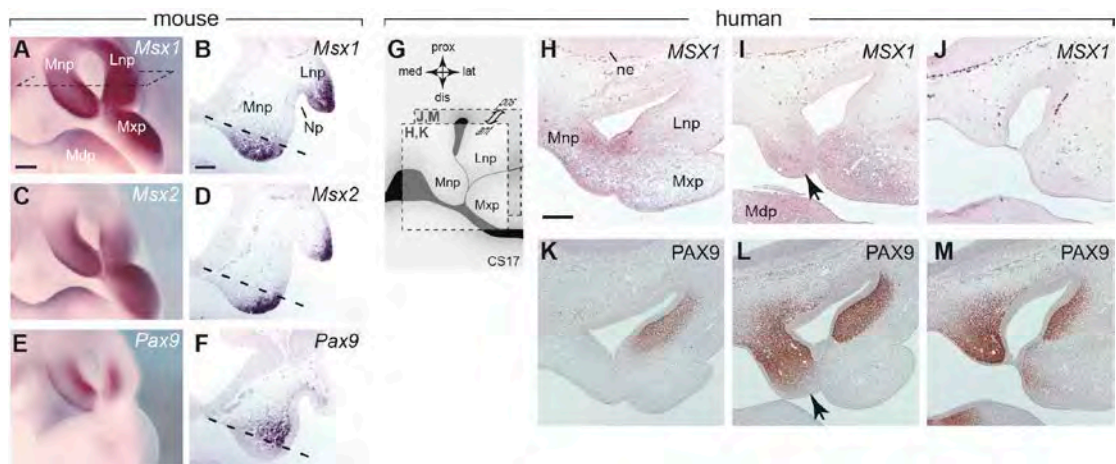
Fig. 2. Conserved complementary expression patterns of *Msx1* and *Pax9* in the Mnp and Lnp in mice and humans

In situ hybridisation of whole mount embryos (**A,C,E**) and on coronal sections (**B,D,F**; plane of section indicated by rectangle in **A**). While *Msx1* and *Msx2* are primarily expressed in the epithelium and mesenchyme of the anterior region of the Mnp (**A-D**), *Pax9* transcripts are mainly detectable in the posterior Mnp mesenchyme (**E,F**). (**G**) Diagram of the developing human nose and lip at Carnegie Stage 17 (CS17). Squares indicate levels of sections used for expression analysis. *MSX1* transcripts detected by *in situ* hybridisation dominate in the anterior regions of the Mnp and Mxp (**H-J**), whereas immunohistochemical staining shows that PAX9 expression is mainly found in the posterior part of the Mnp (**L,M**) and in the mesenchyme adjacent to the nasal epithelium of the Lnp (**K-M**). Abbreviations: Lnp, lateral nasal process; Mdp, mandibular process; Mnp, medial nasal process; Mxp, maxillary process; Ne, neural epithelium. Scale bars: 200μm (A, H), 100μm (B).
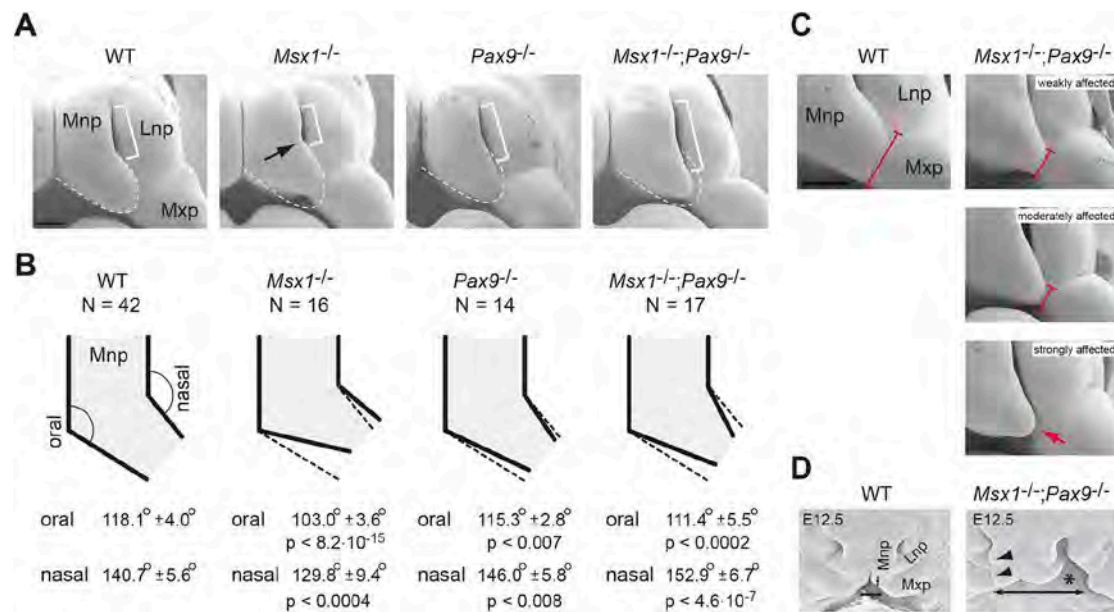
Fig. 3. A *Pax9*-dependent alteration of Mnp morphogenesis prevents cleft lip in *Msx1*^{-/-} mutants.

(**A**) Scanning electron microscopy (SEM) images of the embryonic nose and lip at E11.5. Dashed line delineating the normal shape of the Mnp is superimposed on mutant embryos. A sharp bend of the Mnp is formed in *Msx1*^{-/-} mutants (arrow) and is associated with a shorter nasal pit (bracket). In contrast, the curvature is attenuated and nasal pits are longer in *Pax9*^{-/-} and *Msx1*^{-/-};*Pax9*^{-/-} mutants, respectively. (**B**) Schematic Mnp shapes and angles of oral and nasal aspects. Dashed lines indicate wild-type Mnp angles. Note that the angle on the nasal aspect is smaller in *Msx1*^{-/-} mutants, and bigger in *Pax9*^{-/-} mutants and *Msx1*^{-/-};*Pax9*^{-/-} mutants. *P*-values refer to comparisons with wild-type samples. (**C**) SEM images showing different severities of affected Mnp-Mxp contact in *Msx1*^{-/-};*Pax9*^{-/-} mutants. The zone of contact is consistently reduced (brackets) and absent in some cases (arrow). (**D**) SEM images at E12.5. *Msx1*^{-/-};*Pax9*^{-/-} mutants exhibit a wider distance between Mxps (double arrow). Unilateral cleft lip (asterisk) and incomplete Mnp-Lnp and Mnp-Mxp fusion (arrowheads) are consistently seen in these mutants. Abbreviations: Lnp, lateral nasal process; Mdp, mandibular process; Mnp, medial nasal process; Mxp, maxillary process; WT, wild type. Scale bars: 250μm (B), 200μm (G,M), 100μm (I), 50μm (S).
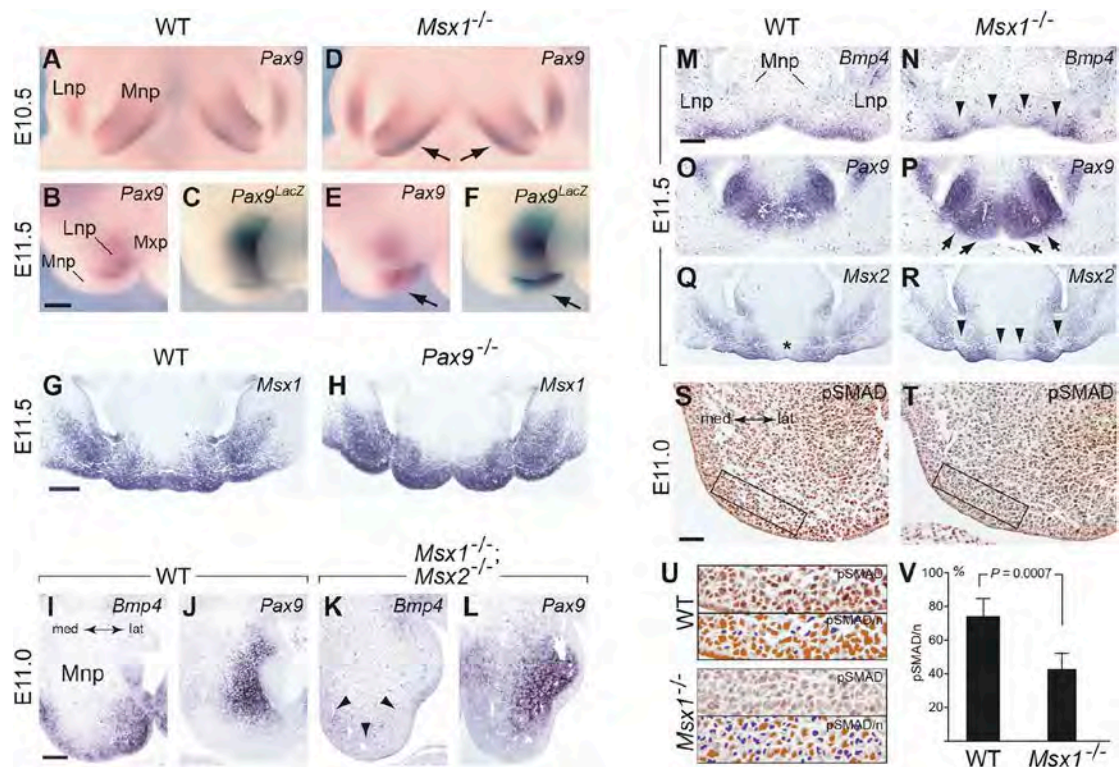
Fig. 4. *Msx1* **and** *Msx2* **modulate the complementary expression patterns of** *Bmp4* **and** *Pax9***.**

Frontal (**A,D**) and lateral (**B,C,E,F**) views of whole mount embryos hybridized to *Pax9* (**A,B,D,E**) or stained with X-Gal (**C,F**). *Pax9* expression is up-regulated in *Msx1*^{-/-} embryos at E10.5 (arrows in **D**), and is expanded distally at E11.5 (arrows in **E** and **F**). (**G,H**) Coronal sections of the nasal region. The expression of *Msx1* is not affected in *Pax9*^{-/-} embryos. (**I-L**) In situ hybridisation of *Bmp4* and *Pax9* in the Mnp. Mesenchymal expression of *Bmp4* is normally restricted adjacent to the epithelium (**I**) and is barely detectable in *Msx1*^{-/-}*;Msx2*^{-/-} embryos (arrowheads in **K**). Conversely, *Pax9* expression is normally restricted to a proximal domain (**J**) and is expanded in the mutants (**L**). (**M-R**) *In situ* hybridization on coronal sections at E11.5. *Bmp4* expression pattern in the distal mesenchyme is interrupted in *Msx1*^{-/-} embryos (arrowheads in **N**). *Pax9* expression is stronger and expanded in *Msx1*^{-/-} embryos and is found in the direct vicinity of the ectodermal epithelium (arrows in **P**). (**Q,R**) Expression of *Msx2* partially overlaps with that of *Bmp4* in both wild-type and *Msx1*^{-/-} embryos. Note that *Msx2* expression is missing centrally in wild-type embryos (asterisk in **Q**) and that *Msx2*-negative areas (arrowheads in **R**) match those at which *Bmp4* is also absent (compare to **N**). (**S-V**) Results of pSmad staining in wild-type and

Msx1^{-/-} embryos. (**U**) Detection of pSmad-positive nuclei (brown) and pSmad-negative nuclei (blue), as determined by ImmunoRatio (see Materials and Methods). (**V**) The ratio of pSmad-positive cells/all nuclei is significantly reduced in Mnp of *Msx1^{-/-}* embryos. Abbreviations: lat, lateral; Lnp, lateral nasal process; med, medial; Mnp, medial nasal process; Mxp, maxillary process. Scale bars: 250μm (A,B), 200μm (C,D).
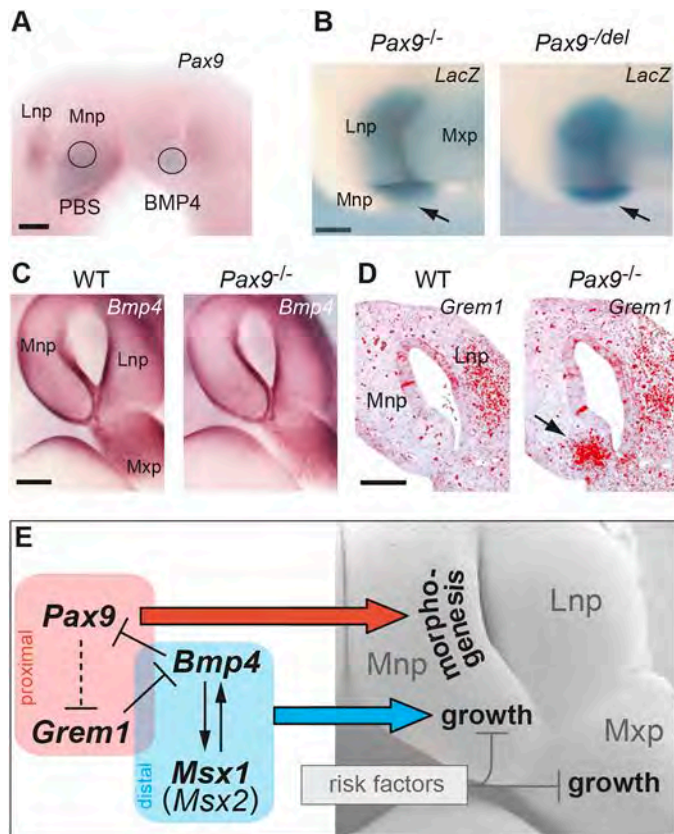
Fig. 5. Mnp development involves a negative *Bmp4-Pax9-Grem1* feedback loop

(**A**) *Pax9* whole mount *in situ* hybridization of embryonic nose and lip after organ culture. Circles mark the positions of implanted BMP4 and control (PBS) beads. *Pax9* expression in both Mnp and Lnp is strongly down-regulated by BMP4.(**B**) Expansion of *Pax9^LacZ^* expression is seen in both *Pax9^-/-^* (two *LacZ* alleles) and *Pax9^-/del^* (one *LacZ* allele) mutant embryos. (**C**) *Bmp4* expression is not altered in the absence of *Pax9* at E10.5. (**D**) *Grem1* is ectopically expressed in the Mnp of *Pax9^-/-^* embryos (arrow). (**E**) Suggested model showing how *Bmp4* may connect a positive feedback loop (*Msx1*, *Msx2* and *Bmp4*) regulating Mnp growth to a negative feedback loop (*Pax9*, *Grem1* and *Bmp4*) involved in regulating Mnp shape. Inactivation of *Msx1* results in a growth defect of the Mnp but also in the increase of *Pax9* expression, leading to a *Pax9*-dependent, compensatory morphogenetic change that prevents cleft lip formation in *Msx1^-/-^* embryos. A cleft lip may form when this compensatory pathway cannot be activated (*Msx1^-/-^;Pax9^-/-^* mutants), or when the growth defect is augmented by an environmental risk factor (*Msx1^-/-^* mutants exposed to hypoxia/phenytoin). Abbreviations: Lnp, lateral nasal process; Mnp, medial nasal process; Mxp, maxillary process. Scale bars: 200 μm.
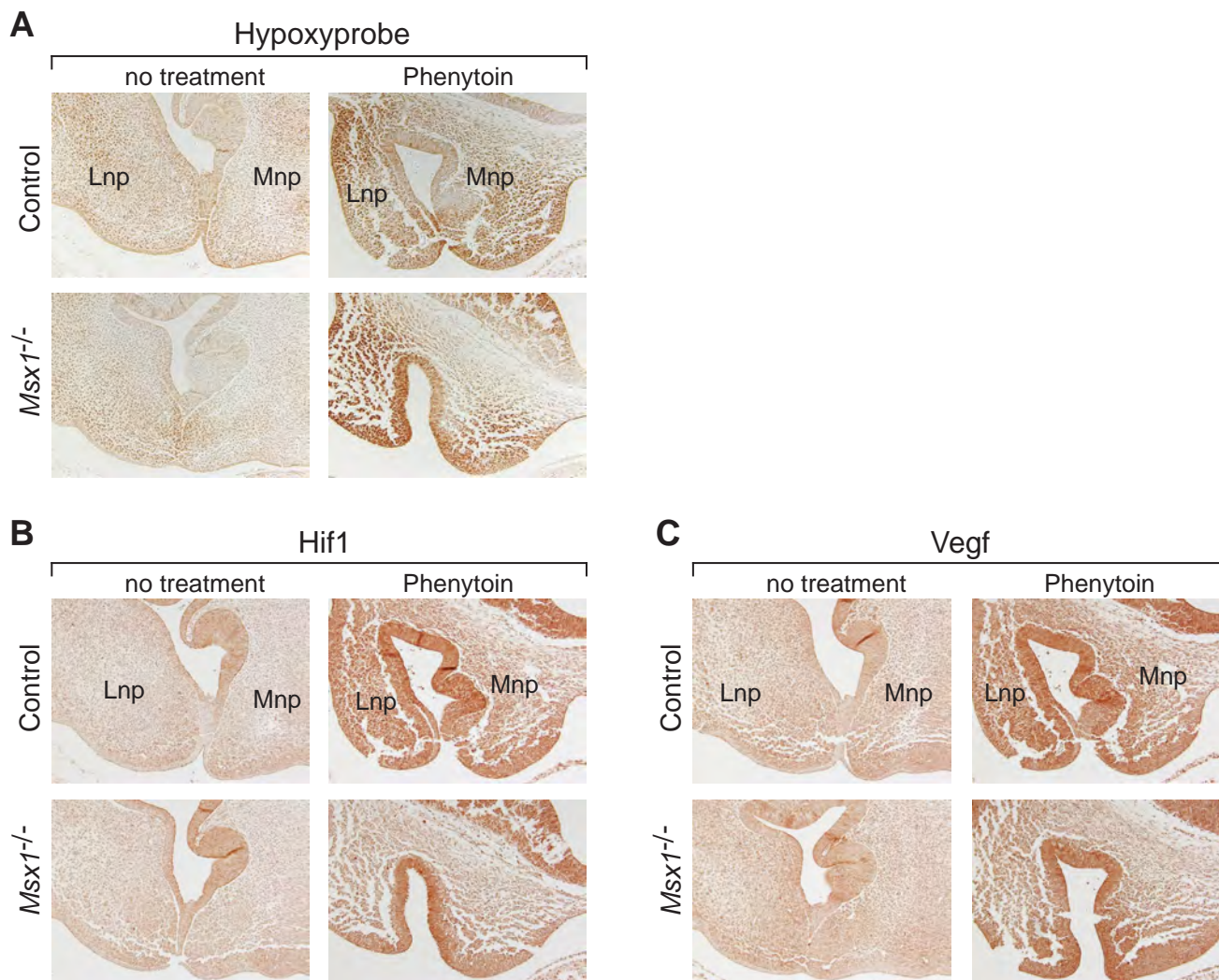
A

B   **C**

Fig. S1. Hypoxia and expression of Hif1 and Vegf in the lip-forming region at E11.0. In the experimental group, Phenytoin was injected at a concentration of 60mg/kg. (**A**) Hypoxic tissue is detectable in the medial nasal process (Mnp) and lateral nasal process (Lnp) of both control embryos and *Msx1^{-/-}* mutants after Phenytoin injection. (**B**) Hif1 expression is induced in the experimental group but is weaker in *Msx1^{-/-}* mutants when compared to that in controls. (**C**) Vegf is expressed after Phenytoin injection and appears stronger in the control embryo.
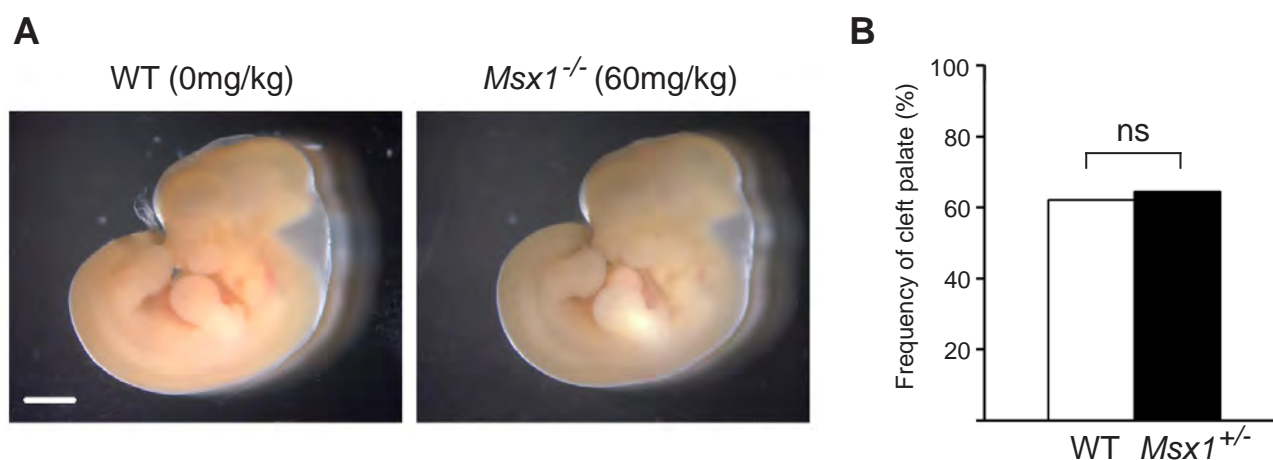
A   **B**

Fig. S2. Interaction between *Msx1* mutation and phenytoin-induced clefting is not influenced by the maternal genotype. (**A**) Lateral view of embryos (E11.5) exposed to phenytoin. Phenytoin injection does not affect general body development even in the complete absence of *Msx1*. (**B**) No significant difference of cleft palate frequencies is seen in phenytoin-exposed *Msx1^{+/-}* embryos from wild-type (N=37) or *Msx1^{+/-}* (N=45) mother, indicating that the genotype of the embryo but not that of the mother is the critical determinant of phenytoin-induced orofacial clefting. WT, wild type; ns, not significant. Scale bar: 1mm.
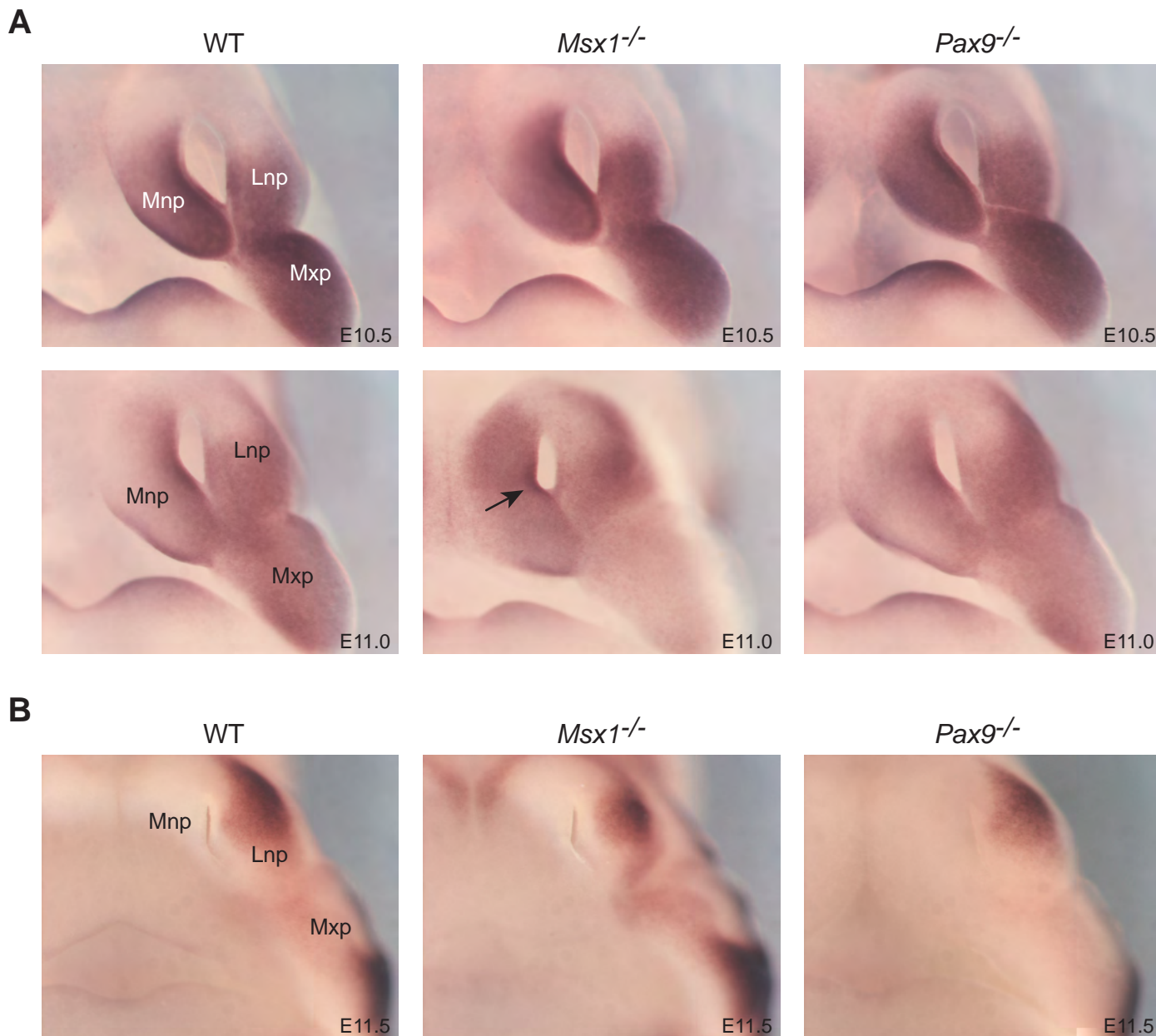
A

B

Fig. S3. Whole-mount in situ hybridization of genes paralog to *Msx1* and *Pax9*. The expression patterns of *Msx2* (**A**) and *Pax1* (**B**) are not changed among wild-type (WT), *Msx1*-/- and *Pax9*-/- embryos, respectively. Note the kink on the nasal aspect of the Mnp in the *Msx1*-/- embryo at E11.0 (arrow).
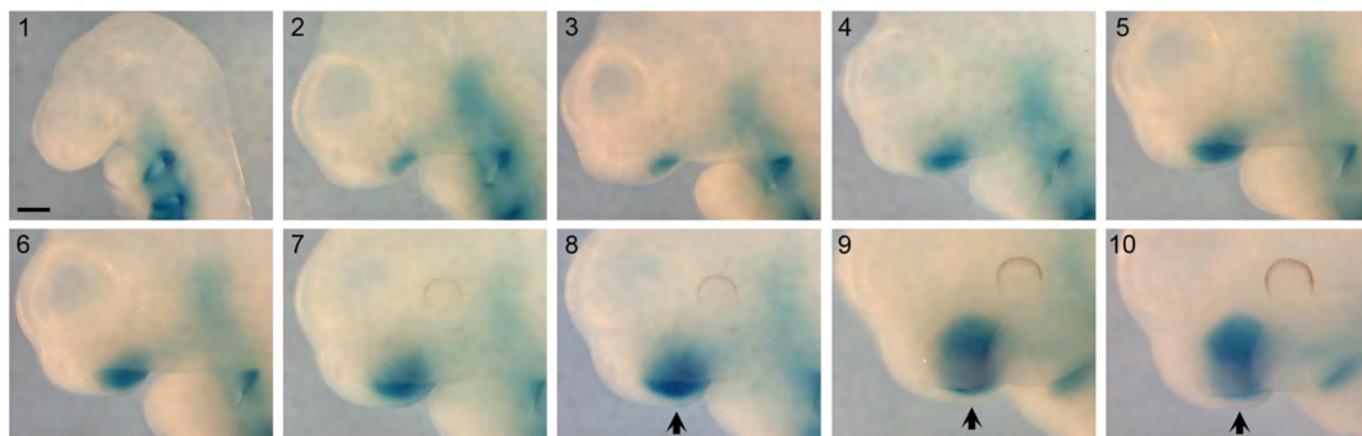

Fig. S4. Pax9 expression is gradually down-regulated in the distal region of the developing Mnp. Lateral view of X-gal stained *Pax9*+/- embryos between E10.0 to E10.75 (arranged in a chronological order and labelled 1-10). Note that at earlier stages *Pax9* is initially expressed at the tip of the Mnp, after which the expression becomes restricted to more proximal regions as development proceeds(arrows). Scale bar: 250 µm.
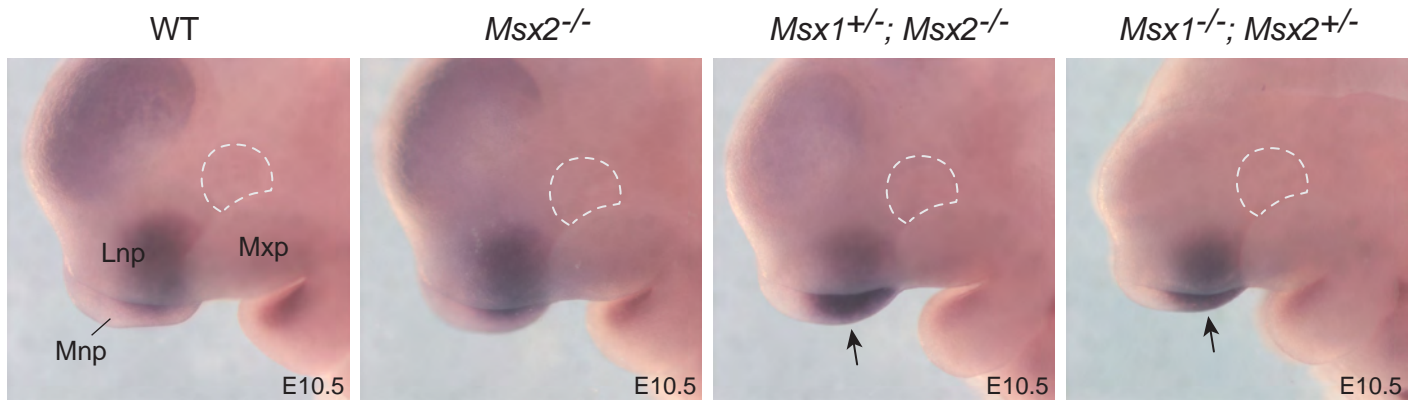
Fig. S5. *Pax9* **expression at E10.5 is expanded in the medial nasal process (Mnp) of** *Msx1/Msx2* **compound mutants.** Images show lateral views; the visible part of the eye is outlined to aid orientation. Note the distally expanded expression of *Pax9* in the Mnp of *Msx1+/-; Msx2-/-* and *Msx1-/-; Msx2+/-* embryos (arrows).

Table S1. Raw data of sample numbers of phenytoin-induced cleft lip and cleft secondary palate. Upper rows indicate phenytoin dosage in mg/kg body weight of the pregnant mother. Note that total numbers of cleft lip (CL) are subdivided into unilateral (U) and bilateral (B) CL, while hypoplastic (H) upper lips were not counted as CL and thus were not considered in the statistical analysis. Numbers of cleft secondary palate (CP) are subdivided into partial (P) and complete (C) clefts and were all considered in the statistical analysis. N = number of embryos analysed; ns = not significant; / = no informative result or sample number to low for statistical analysis.

Click here to Download Table S1

Table S2. Statistical evaluation of pSMAD-positive nuclei in the Mnp of control and *Msx1* [-/-] embryos. In both groups four samples with 6 sections each were analysed using ImmunoRatio (Fig.S6) to determine the percentage of stained nuclei.

Click here to Download Table S2

Table S3. A total of 1073 human genes are annotated in GO:0009887 (animal organ morphogenesis; column A, list retrieved in January 2020). GWAS data analysed by VEGAS Pathway Analysis was available for 632 genes, of which 557 genes could be directly matched to GO:0009887 (shown in grey). 166 out of 557 genes (29,8%) have previously been shown to be involved in human or mouse lip, palate or facial development.

Click here to Download Table S3

Table S4. 75 genes were identified by VEGAS Pathway analysis that are not included in the most recent GO:0009887 (list retrieved in January 2020). 18 out of 75 genes (24%) have previously been shown to be associated with defects in human or mouse lip, palate or facial development.

Click here to Download Table S4

Table S5. Of 112 loci recently identified to be associated with variations in facial morphology 32 genes could be matched to genes listed in GO:0009887 ("organ morphogenesis") that were present in our Vegas Pathway Analysis

Click here to Download Table S5